



Review article

Conductive fibers for biomedical applications

Leqian Wei^{a,b}, Shasha Wang^{a,b}, Mengqi Shan^{a,b}, Yimeng Li^{a,b}, Yongliang Wang^c,
Fujun Wang^{a,b}, Lu Wang^{a,b}, Jifu Mao^{a,b,*}

^a Key Laboratory of Textile Science & Technology, Ministry of Education, College of Textiles, Donghua University, Shanghai, 201620, China

^b Key Laboratory of Textile Industry for Biomedical Textile Materials and Technology, Donghua University, Shanghai, 201620, China

^c School of Health and Life Sciences, University of Health and Rehabilitation Sciences, Qingdao City, Shandong Province, 266071, China



ARTICLE INFO

Keywords:

Conductive fibers

Conductive biomaterials

Tissue repair

Implantable bioelectronics

Wearable bioelectronics

ABSTRACT

Bioelectricity has been stated as a key factor in regulating cell activity and tissue function in electroactive tissues. Thus, various biomedical electronic constructs have been developed to interfere with cell behaviors to promote tissue regeneration, or to interface with cells or tissue/organ surfaces to acquire physiological status via electrical signals. Benefiting from the outstanding advantages of flexibility, structural diversity, customizable mechanical properties, and tunable distribution of conductive components, conductive fibers are able to avoid the damage-inducing mechanical mismatch between the construct and the biological environment, in return to ensure stable functioning of such constructs during physiological deformation. Herein, this review starts by presenting current fabrication technologies of conductive fibers including wet spinning, microfluidic spinning, electrospinning and 3D printing as well as surface modification on fibers and fiber assemblies. To provide an update on the biomedical applications of conductive fibers and fiber assemblies, we further elaborate conductive fibrous constructs utilized in tissue engineering and regeneration, implantable healthcare bioelectronics, and wearable healthcare bioelectronics. To conclude, current challenges and future perspectives of biomedical electronic constructs built by conductive fibers are discussed.

1. Introduction

Bioelectricity is recognized as a crucial instructive factor for human life activities and its regulative actions in cell behavior have been well documented although its action mechanism remains undefined [1]. Numerous *in vitro* and *in vivo* experiments have exerted electrical stimulation to living cells and tissues directly through electrodes or indirectly through bioelectronic devices based on conductive biomaterials, to trigger series of cell activities for tissue repair process in electroactive tissues, such as cardiac [2–5], nerve [6–8], bone [9–12] and skin [13–15]. Furthermore, sufficient evidence suggests that electrical signals can be transmitted by conductive biomaterial graft or bioelectronic devices implanted in or worn on human bodies to activate beneficial electrical response in processes of wound healing [14,15], drug delivery [16], sensing for biochemical factors and biophysical signals for tissue repair [17,18], and health monitoring [19,20]. In such context, conductive biomaterials are highly desirable for conductive scaffolds

and bioelectronics.

Conductive biomaterials, the indispensable components of conductive scaffolds and bioelectronics, have been gaining growing attention and rapid development in recent years. Conductive biomaterials can be generally classified as five categories: (1) intrinsic conductive polymers (ICPs), such as polypyrrole (PPy) [21], polyaniline (PANI) [22], and poly (3,4-ethylenedioxythiophene) (PEDOT) [23]; (2) carbon nanomaterials, including one-dimensional single-walled carbon nanotubes (SWCNTs), multi-walled carbon nanotubes (MWCNTs) [24,25] and carbon nanofibers (CNFs) and two-dimensional graphene, graphene oxide (GO) and reduced graphene oxide (rGO) [26–28]; (3) metallic nanomaterials, such as silver nanoparticles (AgNPs), silver nanowires (AgNWs), gold nanoparticles (AuNPs) and gold nanorods (AuNRs); (4) MXenes, two-dimensional crystal nanomaterials of transition metal carbides, nitrides or carbonitrides, represented by $Ti_3C_2T_x$ nanosheets; (5) liquid metals (LM), represented by eutectic-gallium-indium (EGaIn) [29,30]. Each type of conductive biomaterials possesses their own

Peer review under responsibility of KeAi Communications Co., Ltd.

* Corresponding author. Key Laboratory of Textile Science & Technology, Ministry of Education, College of Textiles, Donghua University, Shanghai, 201620, China.

E-mail address: jifu.mao@dhu.edu.cn (J. Mao).

<https://doi.org/10.1016/j.bioactmat.2022.10.014>

Received 30 June 2022; Received in revised form 12 September 2022; Accepted 7 October 2022

2452-199X/© 2022 The Authors. Publishing services by Elsevier B.V. on behalf of KeAi Communications Co. Ltd. This is an open access article under the CC BY-NC-ND license (<http://creativecommons.org/licenses/by-nc-nd/4.0/>).

unique advantages applicable to biomedical constructs, yet at the same time, most of them also display an inevitable disadvantage, i.e., mismatched mechanical behaviors with the deformable tissues leading to severe inflammation and electronic failure [31,32]. Fortunately, as a special form of soft materials, fibers and fiber assemblies are equipped with lightweight, distinguished flexibility, tunable mechanical properties and structural diversity. Consequently, with reasonable composition and structure design of conductive fibers and mature weaving, knitting, braiding, embroidering, stitching, and nonwoven technologies, it is readily to meet the requirements of multidimensional deformation capacity under complex forces and biomimicking heterogenous structures for biomedical constructs [33,34]. In order to maximize the advantage of these conductive biomaterials in biomedical applications, great effort has been put in the researches of fabrication and applications of conductive fibers.

Herein, this review mainly focuses on flexible composite conductive fibers aimed at biomedical field. Fabrication methods of conductive fibers with enriched composition/structural designs are concluded as wet spinning, electrospinning, microfluidic fabrication, 3D printing, and surface modification on fibers, yarns or fabrics. Current advances of conductive fibers applied in tissue repair and regeneration for electroactive tissues, implantable bioelectronics and wearable bioelectronics for personal health monitoring are discussed separately. Finally, existing issues and prospects for further development of conductive fibers are provided as well.

2. Fabrication technologies for conductive fibers

Due to the inherent rigidity, insolubility and infusibility of most conductive biomaterials, preparation of composite conductive fibers is usually chosen for the feasibility, flexibility and convenience of processing [35]. The mechanical, electrical and biological properties can be

fine-tuned by proper composition and structure designs of fibers to meet the requirements of tissue repair materials or bio electronics. Hence, various types of conductive fibers have been developed by the combination of fiber-forming polymers and conductive biomaterials through wet spinning, microfluidic spinning, electrospinning and 3D printing, as well as through surface modification on nonconductive fibers. Moreover, textile processing technologies are further adopted to enrich structure designs of conductive fibers to obtain biomimicking structures.

2.1. Fiber fabrication technology

2.1.1. Wet spinning

Wet spinning is a mature filament production technology for soluble/dispersible materials (Fig. 1A), in which homogeneously dispersed spinning dope is continuously injected into a certain poor solvent of the solute through a syringe with a fine needle driven by an injection pump [19]. After the nonsolvent-induced phase separation, the thin flow is solidified and subjected to drying and/or stretching to obtain fibers. Among all the general spinning parameters of solvent, concentration and flow rate of the precursor solution, needle diameter, solvent, temperature and concentration of the coagulation bath, and solidification time, the used solvents crucially affect formation of stable spinning flow and smooth double diffusion process.

Uniform distribution of conductive components in fibers ensures the consistent mechanical and electrical properties in different segments along the fiber, and avoids severe interface issue due to the typical mechanical mismatch. Therefore, to weaken the strong interactions of the conductive nanoparticles, the solvent systems and mixing means are considered to form stable spinning solutions. Thorough stirring was adopted to mix CNTs and MXenes uniformly with polyurethane (PU)/dimethyl formamide solution, and after being injected into the coagulation bath, a stretchable conductive fiber was prepared [36]. With the

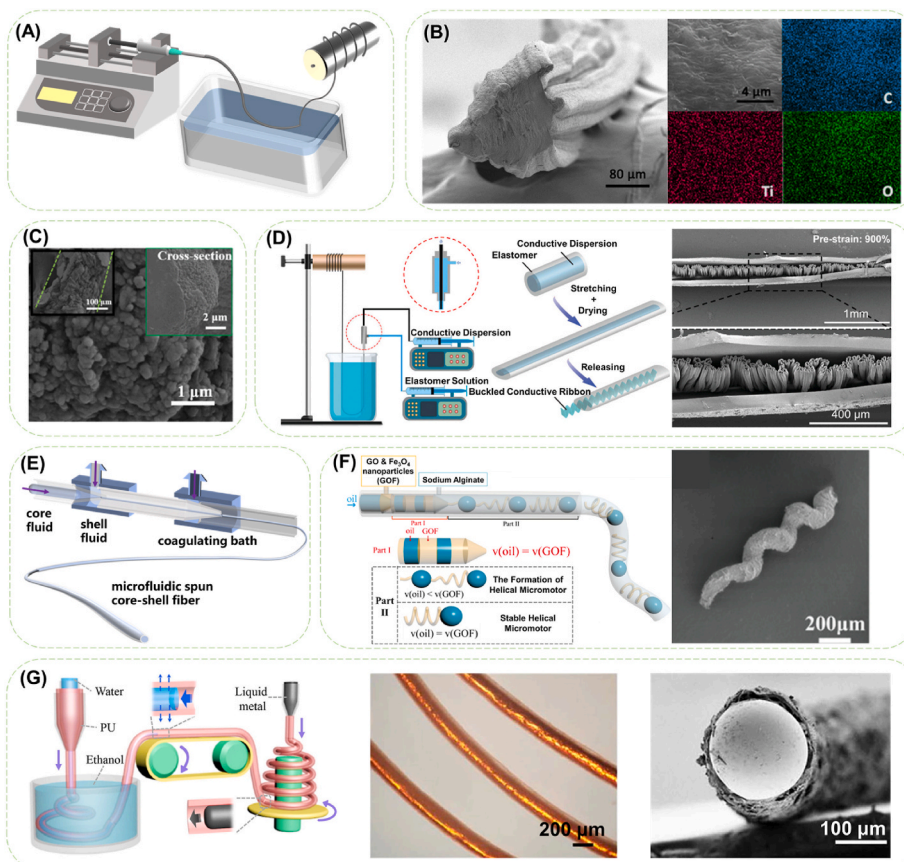


Fig. 1. Diagrams of conductive fibers fabricated by wet spinning and microfluidic spinning. (A) Typical fabrication device for wet spinning process. (B) Cross-sectional SEM image and EDS mapping images of C, Ti, and O of the MXene/CNT/PU fiber. Reproduced with permission from Ref. [36]. Copyright 2021, Elsevier Ltd. (C) SEM image of corn-like PANi-regenerated cellulose fiber. Reproduced with permission from Ref. [37]. Copyright 2016, American Chemical Society. (D) The coaxial wet-spinning process for encapsulating the conductive dispersion in an elastic TPE channel and the pre-strain-then-buckling strategy and SEM image of the obtained fiber fabricated with 900% pre-strain. Reproduced with permission from Ref. [38]. Copyright 2019, WILEY-VCH Verlag GmbH & Co. KGaA, Weinheim. (E) Schematic illustration of microfluidic spinning process. (F) Schematic diagram of the formation mechanism and the SEM image for the graphene oxide-based helical micromotors (GOFHMs). Reproduced with permission from Ref. [39]. Copyright 2020, American Chemical Society. (G) Schematic illustration of the generation device of the LM-encapsulated microfiber, and the bright-field microscopic image and the SEM image of the cross-section of LM-encapsulated microfibers. Reproduced with permission from Ref. [40]. Copyright 2020, Science China Press.

MXene nanosheets serving as the connecting bridges among the CNT network (Fig. 1B), the composite fiber achieved an optimized conductivity of $\sim 6 \text{ S cm}^{-1}$ under 200% strain with a combined CNT concentration of 4 wt% and MXene concentration of 0.5 wt%. In order to ensure the biocompatibility while overcoming the poor dispersion of graphene in aqueous system, a surfactant-free strategy was proposed by simple mechanical stirring graphene/cellulose aqueous solution with a mediation of inorganic alkali [41]. The steric hindrance effect between the inorganic metal-ions loaded on graphene and the cellulose chains could effectively prevent the π - π stacking of nanosheets leading to stable cellulose/graphene aqueous spinning dope. The densified hydrogen bonds between graphene and cellulose with a 5 wt% graphene granted the composite fiber ductile fracture behavior (fracture strain: $11.1 \pm 0.6\%$, toughness: $17.9 \pm 0.4 \text{ MJ/m}^3$) and a conductivity of $0.51 \times 10^{-2} \text{ S cm}^{-1}$.

The process of mutual diffusion, infiltration and exchange between the spinning solution and coagulation bath also matter to the properties of the obtained fibers. The tensile behavior of polystyrene sulfonic sodium (PSS) doped PEDOT (PEDOT:PSS)/polyvinyl alcohol (PVA) fiber was found to be affected by both the formation of stably entangled molecular chains and the phase transition process [42]. In this case, PVA could disrupt the electrostatic complexation between PEDOT and PSS molecular chains, and therefore the entangled PVA and PEDOT molecular chains can increase the breaking elongation. On the other hand, ethylene glycol could smooth the structure of the PEDOT molecular chains, rendering strengthened PEDOT fibers. Peak breaking strength and elongation ($180 \pm 6.1 \text{ MPa}$ and $32 \pm 1.7\%$, respectively) were reached at 20 wt% PVA and the addition of 10 wt% ethylene glycol in the PEDOT:PSS/PVA solution further increased the strength to $210 \pm 5 \text{ MPa}$. Moreover, enhanced elongation and conductivity of wet spun fibers can be also effected by alteration in coagulation bath. With the assistance of the electrostatic complexation between PSS and metal ions, rapid gelation of PEDOT:PSS was enabled in an environment-friendly and low-cost coagulation bath of water-ethanol [43]. Pure PEDOT:PSS fiber prepared with 0.1 M Li^+ in the water-ethanol bath achieved a maximal elongation (55%) and a highest conductivity ($\sim 10 \text{ S cm}^{-1}$) compared with addition of other metal ions with different valences.

Structure designs of wet spun fibers can be implemented by different means, such as *in situ* polymerization of ICPs in the coagulation bath, coaxial feeding of spinning solutions, and adjusting drawing speed of the spinning flow. Corn-like PANi/regenerated cellulose fiber was prepared by *in situ* polymerization of aniline in the oxidant-contained coagulation bath (Fig. 1C) [37]. Stretchable coaxial fiber with buckled PEDOT:PSS cores were prepared through coaxial wet spinning of thermoplastic elastomer (TPE) solution and PEDOT:PSS/polyethylene-block-poly (ethylene glycol) (PBP) solution while stretching the solidified TPE fiber before drying (Fig. 1D) [38].

Despite the relatively simple and industrially scalable process, it is difficult to realize precise regulation over the fluid and control over the fiber-forming process especially when it comes to multi-phase fluid. Besides, the decision and application of the spinning aid and the coagulation bath can cause worrisome biotoxicity, environmental pollution and waste. Although some concepts of green wet spinning have emerged, circumspect consideration should be put in the whole situation of such wet chemistry.

2.1.2. Microfluidic spinning

By precisely integrating multiphase concentric/laminar flows and regulating the flowing state of each phase in separate microchannels, well-defined microscale fibers can be fabricated by microfluidic devices [44]. The most basic form of microfluidic spinning consists of two fluid phases forming a coaxial configuration with a core fluid hydrodynamically focused by the sheath fluid in the channel (Fig. 1E). When the core flow is solidified *in situ* by ultraviolet (UV)-induced polymerization, phase inversion, ionic or chemical cross-linking, thermal curing, or solvent evaporation [45], fibers can be extruded through an outlet

channel without clogging due to the lubrication action of the sheath flow.

Owing to the controllable adjustment of spinning parameters during microfluidic fabrication and easy modification of microfluidic devices, composite fibers with desired structure designs can be prepared. Wu et al. [46] prepared an oriented GO/polyacrylonitrile (PAN) composite fiber membrane by microfluidic spinning with a moving receiver using an orthogonally optimized parameter combination of the PAN concentration (15%), flow rate (0.5 mL/h), and rotation speed of the receiving frame (200 rpm). The degree of orientation of the composite membrane was further improved to 89.3% after stabilization and carbonization. Hollow fibers composed of alginate, polyacrylamide (PA), and PPy were prepared through Ca^{2+} ion crosslinking at the intersection of the microfluidic channels followed by UV crosslinking of PA [47]. The lumen size of the composite fiber could be regulated from $\sim 0.8 \text{ mm}$ to $\sim 1.2 \text{ mm}$ by varying external and internal nozzle diameter, while the wall thickness could be increased from $\sim 0.1 \text{ mm}$ to $\sim 0.3 \text{ mm}$ with varied external and internal flow rate. Such tunable lumen morphology and a biologically compatible conductivity of $\sim 3 \times 10^{-3} \text{ S cm}^{-1}$ provided both structural and characteristic basis for drug loading and bioelectrical signal transduction. Moreover, functionalized helical microfiber can also be fabricated by utilizing the unbalanced fluidic friction between the microfiber and its surrounding fluid, adjusting the flow rates of fluids or varying the structures of microfluidic devices [39, 48–50]. Magnetic microscale coils were formed within the optimized concentration range of graphene oxide/ Fe_3O_4 (GOF) solution (16–22 wt %) and sodium alginate (SA) solution (1.5–3.5 wt%), meanwhile the pitch (254.2 – $1107.7 \mu\text{m}$), length, and linear diameter can be tailored by adjusting the flow velocity of GOF solution, the oil phase and the SA solution (Fig. 1F) [37].

Additionally, parameter adjusting and device modifying are in favor of optimizing fiber properties. LM-encapsulated PU microfibers with adjustable conductivity and good deformation ability (480%) were constructed by coaxially injecting PU (1–5 mL/h) and LM (0.1–0.5 mL/h) in the opposite direction with a speed difference in feeding flow (Fig. 1G) [40]. Lam et al. [51] designed a coaxial microfluidic device with an external Teflon tube for the water coagulant solution of calcium chloride and acetic acid, and an internal glass tube for the aqueous mixture of natural rubber, CNTs, and PEDOT:PSS. Upon neutralization of the negative charge of the rubber by Ca^{2+} , continuous fibers with an elongation rate over 1500% were prepared. Due to the addition of PEDOT, the connection of CNTs can be strengthened, resulting in the improved electrical conductivity (33.4 k Ω), linearity (up to 1000%) and durability (200% over 2000 repetitive elongation cycles) of the fibers.

Microfluidic spinning shows obvious advantages of diverse structure designs, easy combination with different crosslinking forms, compatibility with most water-soluble natural polymers and thus reduced difficulty of post-processing and toxicity, which is of great significance to materials for regenerative medicine and tissue engineering. However, since the regulation over the fluid is completed in the confined microscale channels with enhanced surface effect, a noteworthy influence of the surface characteristics of the microchannels on the fluid behavior should be taken into concern. Besides, the difficulty in designing, manufacturing, using and maintaining the microfluidic devices and the relatively low production efficiency of microfluidic technology cannot be neglected.

2.1.3. Electrospinning

Solution electrospinning is a conventional manufacturing technology for micro/nanoscale fibers, the size, morphology and structure of which are comprehensively affected by multiple factors including solution parameters, device parameters and environmental parameters. Since nanomaterials tend to clog the syringe needle or reduce the solution homogeneity and destabilize the Taylor cone [52,53], electrospinning of conductive biomaterials is usually accomplished through mixed dispersion of spinnable polymers and conductive materials (Fig. 2A). By

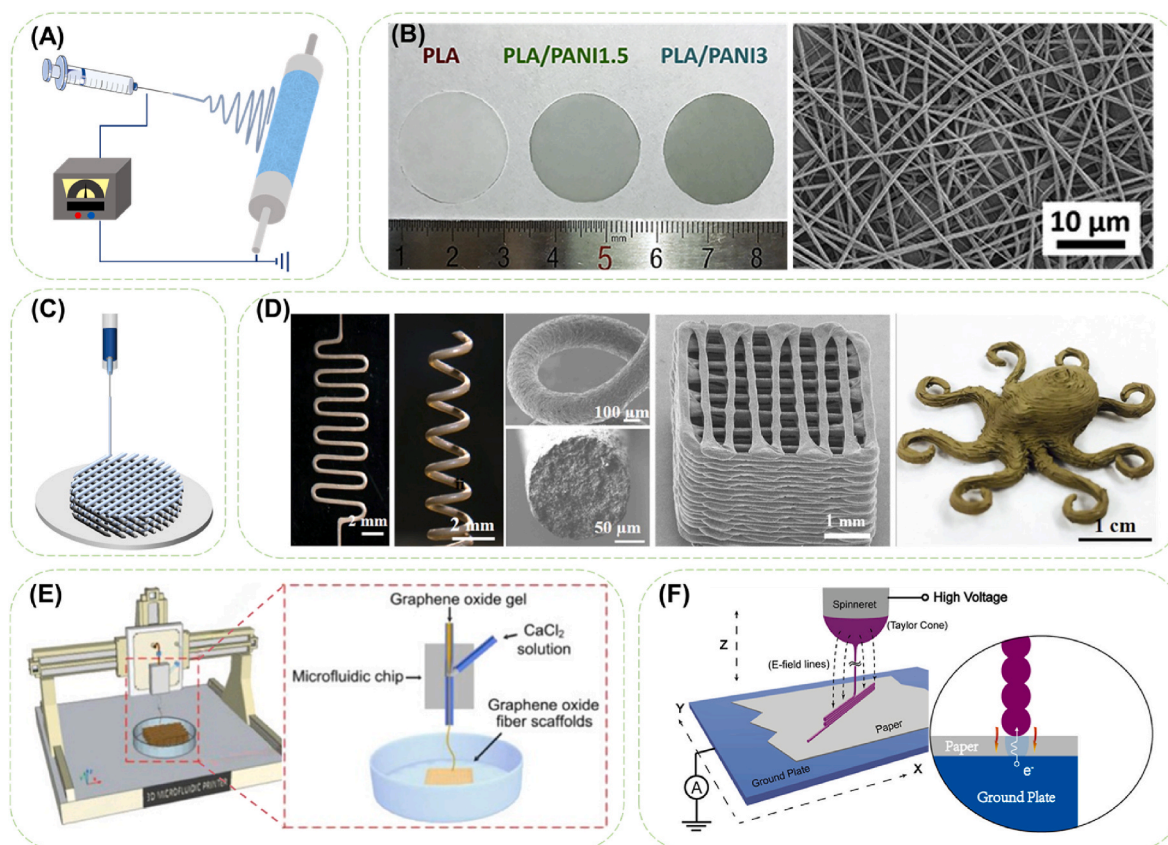


Fig. 2. Diagrams of fabrication of conductive fibers assemblies. (A) Schematic illustration of electrospinning process. (B) Optical images of PLA/PANI nanofibrous sheets with PANI concentrations of 0 wt%, 1.5 wt%, and 3 wt%, and SEM image of PLA/PANI nanofibrous sheets with 3 wt% PANI. Reproduced with permission from Ref. [58] Copyright 2017, Acta Materialia Inc. (C) Schematic illustration of 3D printing process. (D) 3D-printed Ag@CNF/PLA conductive structures including planar zig-zag, freeform 3D spiral, simple layer-by-layer 3D cubic scaffold and complicated self-supported 3D octopus. Reproduced with permission from Ref. [59]. Copyright 2019, American Chemical Society. (E) Schematic setup of the near-field electrospinning process and a close-up schematic of stacked fibers. Reproduced with permission from Ref. [60]. Copyright 2015, American Chemical Society. (F) Schematic illustration of the M3DP for fabricating microfibrillar scaffolds. Reproduced with permission from Ref. [61]. Copyright 2020, American Chemical Society.

involving a sacrificial phase in the spinning solution, single-component electrospun conductive fibers could be obtained, but it always comes with the disadvantages of rigidity, brittleness and higher biological toxicity [54,55].

Optimized composition formula presents a convenient solution to improve the spinnability and reduce the brittleness of the composite fibers. Liang et al. [56] successfully prepared PPy-loaded electrospun silk fibroin (SF) fibers through electrostatic interaction between the negative charged amorphous region of SF and positively charged doped PPy. The addition of PPy reduced the average fiber diameter to $0.375 \pm 0.077 \mu\text{m}$, since conductive jet flows are subjected to stronger drafting force in high-voltage electric field than nonconducting ones. Meanwhile, the existence of 7% SF in the solution granted the fiber mats more uniform distribution of PPy and a reduced Young's modulus ($1.437 \pm 0.044 \text{ MPa}$). Nazari et al. [57] synthesized rGO/Ag nanocomposites and mixed them with PU solution for electrospinning. The existence of AgNPs in electrospun fibers could lead to a lower level of cytotoxicity while rGO could inhibit the agglomeration of AgNPs.

The shapes, diameters and aggregation forms of the conductive fibers can be easily adjusted through altering electrospinning parameters [62, 63]. Aligned fibers with anisotropic mechanical properties can be collected from a disc collector rotating at a speed of 1000 rpm [64]. Fiber sheets with electrical conductivity and nanofibrous structure for cardiac tissue engineering (CTE) were obtained by electrospinning mixture of poly (L-lactide) (PLLA) and PANI (Fig. 2B) [58]. In order to simulate the nanofiber structure of myocardial extracellular matrix (ECM), the diameters of these nanofiber sheets were controlled in the

same range about 500 nm by adjusting the electrospinning voltage of 12–16 kV.

Despite the advantages of wide adaptability of materials, tunable fiber fineness, and simple and adjustable device construction, electrospinning still puts up with challenges of susceptibility to environment change and toxic solvent involvement. On the other hand, the distinguished fiber-forming process of electrospinning also decides that fibers are deposited into compact 2D membranes/mats instead of treatable single fibers. Accurately constructing fiber assemblies with designated complex structures remains as a challenge and warrants further research for electrospinning.

2.1.4. 3D printing

3D printing is an attractive strategy for customizing 3D constructs by extruding melt or solution from the nozzle according to the program-established action trajectory [65,66] (Fig. 2C). Because of the programmability of the additive manufacturing method, it has also been widely used to customize fine-shaped fibers [67,68]. When it comes to fabricating conductive constructs with 3D printed fibers for biomedical applications, the conductive ink has to meet the requirements of certain fluidity (i.e. shear thinning rheological properties) [65], and rapid curing performance [69] to achieve printability, as well as relatively small shear stress for preventing cell damage when extruding cell-laden conductive fibers [70].

Ink components and shear force are both significant to the rheological behavior of conductive ink. In order to prepare elastic conductive fibers, suitable rheological behavior of conductive ink for direct ink

writing was obtained by mixing PTFE powder with polydimethylsiloxane (PDMS) prepolymer to overcome the low viscosity of PDMS [71]. Based on this, coaxial stretchable graphene fibers were successfully prepared with an improved tensile modulus of 120 kPa, a tensile strength of 220 kPa and a length at break of 350%. By introducing amphiphilic nanofibrillated cellulose (NFC), agglomeration of CNTs caused by strong van der Waals force can be overcome in aqueous solution (Fig. 2D) [59]. Obvious shear-thinning behavior of the CNT/NFC solution can therefore be attained, and under the shear force during extrusion and the tension applied during drying, highly arranged conductive microfibers were prepared [72].

To further widen the applicability in heterogeneous bionic structure design, 3D printing has been combined with other spinning methods. Near-field electrospinning (NFES, Fig. 2E), as a combination of 3D printing and solution electrospinning, was established to obtain direct, continuous, and controllable fibers with a minimal line width of 50–500 nm by shortening the distance between needle and collector to 500 μm to 3 mm [73–75]. Melt electrowriting (MEW) is another thriving direct writing technology based on melt-extrusion 3D printing and melt electrospinning, with a fiber diameter ranging from $\sim 2 \mu\text{m}$ to $\sim 50 \mu\text{m}$ [76, 77]. Since MEW requires fusible and thermally stable materials like polycaprolactone (PCL) and high amount of additives leads to poor spinnability or morphology, it remains challengeable for fabricating composite conductive fibers. In Chung's research [78], although composite graphene/PCL fiber was fabricated through MEW, the compromises in printing parameters (printing temperature of 100 $^{\circ}\text{C}$ and minimum printing speed of 30 mm/s) made due to the addition of

graphene resulted into extended cooling time and indistinct layer formation. By combining microfluidic spinning with programmable 3D printing platform, microfluidic 3D printing (M3DP) (Fig. 2F) was developed to fabricate a 3D GO microfibrinous scaffold [61]. After hydrothermal reduction, rGO scaffolds with a conductivity of $2 \times 10^{-3} \text{ S cm}^{-1}$ and adjustable fiber structure can be used for electroactive tissue regeneration. Wei et al. [79] designed a bionic microfluidic printer head to alleviate the problem of gel curing at the nozzle, so that hydrogels can be continuously printed into fibers, two-dimensional networks, and even three-dimensional structures.

3D printing can realize precise control of fiber shapes and especially stack patterns of conductive fibers [80], but it is only available for the polymers with low melting-point or photocuring feature. This restriction on raw materials makes it difficult to meet large-scale industrial production. In addition, it is difficult to accurately control the parameters such as material hydrodynamics and curing time.

The as-mentioned fiber-forming methods are all widely applied in fabricating composite fibers in recent biomedical researches with respective characteristics. On the one hand, wet-spun fibers and electrospun membranes are equipped with tunable structures, predictable mechanical and electrical properties, simple and easily maintainable manufacturing devices, and high preparation efficiency, which are applicable for conforming with the complex deformation of human bodies as components of scaffolds and bioelectronics. On the other hand, microfluidic spinning and 3D printing possess outstanding advantages of precise control over multi-phase fluid and fiber deposition, which is practically useful for constructing multiscale and heterogeneous

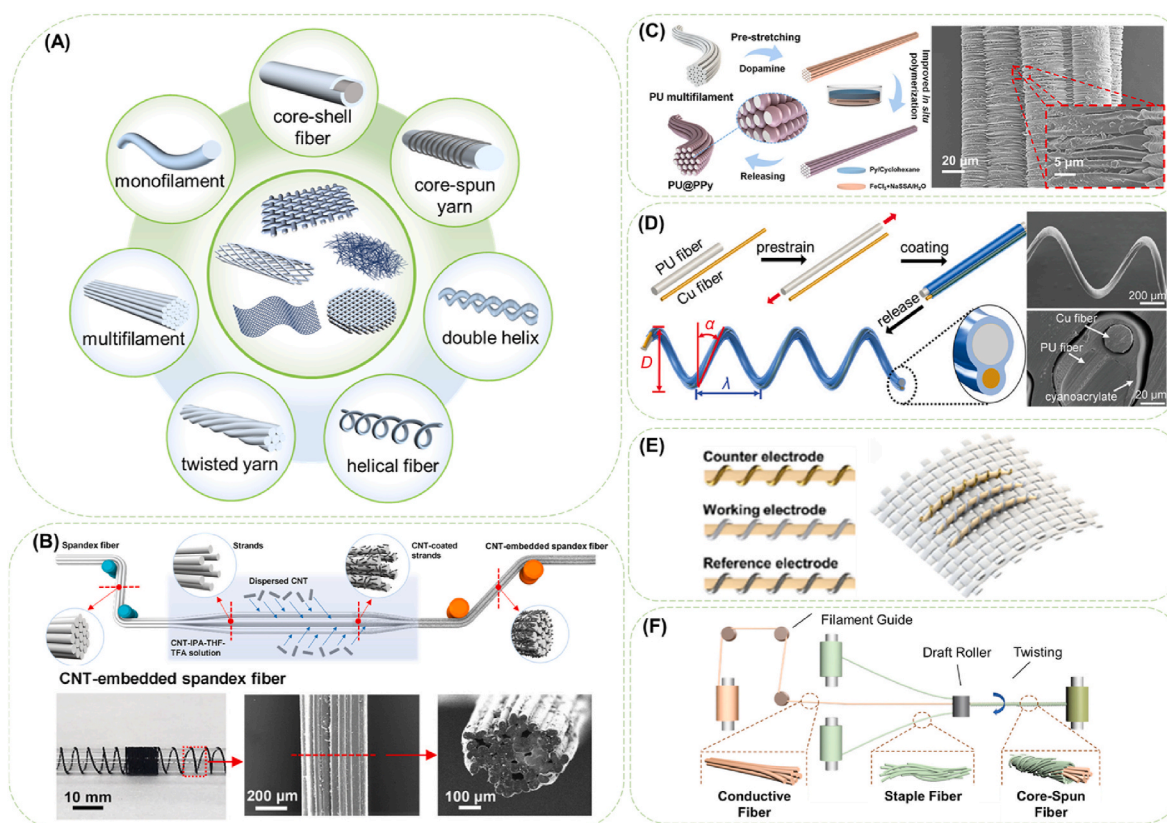


Fig. 3. Diagrams of surface modification for conductive fibers. (A) Different forms of fibers and fiber assemblies. (B) Schematic diagram of the fabrication process of CNT-embedded spandex fiber and photograph and SEM images of the obtained fibers. Reproduced with permission from Ref. [81]. Copyright 2021, American Chemical Society. (C) Schematic diagram of preparing worm-shaped graphene-coated filaments and SEM images of the fiber. Reproduced with permission from Ref. [82]. Copyright 2022, The Authors. Creative Commons Attribution 4.0 International License. (D) Schematic illustration of fabricating helical PU/Cu fibers by fixing a pre-stretched PU fiber and a paralleled Cu fiber and SEM images of the obtained fiber. Reproduced with permission from Ref. [83]. Copyright 2020, WILEY-VCH Verlag GmbH & Co. KGaA, Weinheim. (E) Schematic illustration of the fiber-shaped three-electrode glucose sensor integrated into an elastic textile. Reproduced with permission from Ref. [84]. Copyright 2019, American Chemical Society. (F) Fabrication method of core-spun yarn. Reproduced with permission from Ref. [85]. Copyright 2021, American Chemical Society.

biomimicking structures as integrated multifunctional materials for electroactive tissues.

2.2. Surface modification on fibers

Different from the above-mentioned blending preparation methods, surface modification is a relatively simple and versatile approach for fabricating conductive fibers (Fig. 3A), which can be easily accomplished by modifying process and equipment for dyeing and finishing [33].

Dip coating, spray coating and *in situ* chemical deposition [86,87] are widely applied to simply grant fibers conductivity [88]. Interconnected conductive network of CNTs can form on the fiber surface after immersion in well dispersed CNTs solution (Fig. 3B) [89]. *In situ* polymerization of ICPs can be directly carried out on the surface of fiber substrates to achieve a tight and effective bonding between the conductive layer and the substrate, which is mostly suitable for preparation of conductive fibers with ICPs [62,90–93]. Fibers soaked in pyrrole and *p*-toluene sulfonate solution can be deposited with a 150 nm-thick PPy layer after adding ferric chloride solution for oxidation polymerization [94]. Besides the dispersion status and deposition form of the conductive components, functional groups were introduced on utilized to promote the formation of a continuous conductive layer. For chemically inert raw materials, pre-treatment of surface activation such as amino-silanization treatment [95] or polydopamine (PDA) modification [88] is required for fixed deposition of conductive materials.

Even though effective bonding between the conductive components and the fiber surface can be realized by as-stated modification methods, the huge difference in mechanical properties (especially tensile elongation) will inevitably deactivate the conductive element under physiological deformation. Therefore, serpentine structures, mesh structures, pre-strained wavy structures, and buckling structures have been involved in structure designs of conductive fibers [96], with the same principle of reserving extra length/volume for the intrinsically rigid conductive components when the elastic matrix is undeformed [38,83,97]. Deposition of conductive components on pre-stretched substrates or constructing helix-structured conductive fibers turn out to be the easiest and most useful approach to develop elastic conductive fibers. By wrapping oriented CNT sheets on the stretched styrene (ethylene-butylene)-styrene (SEBS) rubber fiber cores, Liu et al. [98] created highly stretchable (up to 1320%) core-sheath conductive fibers. Muscle fiber bundles-inspired parallel conductive monofilaments were designed by *in situ* polymerization of PPy on pre-stretched PU multifilament, which attained a flexible conductive layer by doping PPy with plasticizer (Fig. 3C) [82]. Differentiated process of strain relaxation of the elastic PU fiber and plastic Cu fiber was utilized to fabricate helical PU/Cu fibers by fixing the pre-stretched PU fiber and a paralleled Cu fiber with cyanoacrylate coating (Fig. 3D) [83]. Similarly, pre-stretching can be implemented on fiber mats by depositing elastic fibers on a sacrificial inelastic matrix with a subsequential removal process of the matrix. Following the strategy, a stretchable Au-deposited fiber mat was developed by electrospinning fluorine rubber on a PSS layer followed by gold sputtering, which can maintain conductive under 170% strain and gas-permeable after an isotropic shrinkage in area of 35–40% on removal of the PSS layer [99].

It is a simple and efficient method to obtain conductive fiber by surface coating, and the surface conductivity of the fiber can be realized by changing the coating parameters. Faced with the possible wet condition and repetitive external force in diverse practical application scenarios, the bonding firmness between the fiber and conductive coating and the conductive stability should be paid more attention. The combined strategy of surface modification and structure design surfaces as a potential solution for preserving conductivity in a larger strain range.

2.3. Assembly technologies of conductive fibers

Taken the axial directions and axial length of fiber assemblies into concern, filaments/fibers/yarns with length of meters to kilometers and nano/microscale diameter can be classified as 1D materials [33], while 2D fiber assemblies mainly refer to electrospun fibrous networks with negligible thickness in this review and 3D fiber assemblies refer to woven fabrics, knitted fabrics, braided wires, tubular braid, and multi-layered 3D printed constructs which contains fiber interlacing or loop intermeshing. Benefitting from the distinctive deformability and combination diversity of 1D fibers, customized conductive fiber assemblies can be fabricated by weaving, knitting, braiding or simply sewing (Fig. 3E) [84] in accordance with the application scenarios and functional requirements.

Yarns possess better loading capacity of conductive components, and the directional arrangement of the fibers in the yarn allows for enhanced mechanical strength and ease of handling. Core-spun yarns stand for a special form of fiber assemblies with the structure of sheath fibers entangled on elastic core filament. Through a proper design of the core filaments and sheath fibers, the properties of obtained core-spun yarns, including high strength, multifunction and wearing comfort can be optimized, meanwhile the high compatibility and strong liquid adsorption capacity can be maintained. Yang et al. [85] wrapped cotton fibers on Ag yarn to form a core-spun yarn (Fig. 3F) and dip-coated with PDMS afterwards to obtain a conductive composite fiber. The composite fiber was able to be further woven into a flexible 3D sensing fabric.

According to the physiological and biophysical principles, conductive fiber-based biomaterials with 2D topography and 3D geometry have been developed to modulate cell behaviors and tissue/organ functions [100]. For bioelectronics, sufficient contact area and deformation conformability between surfaces of the electronic device and the applied tissue/organ are vital for its function implementation. The stretchability of bioelectronics could be realized by adopting either intrinsically stretchable electrode materials or extrinsically stretchable structures, in order to alleviate the strain-related changes in conductivity and active surface of the electrodes. Gao et al. [42] choose nylon coated spandex and PEDOT:PSS/PVA fibers as common and inductive zone yarns respectively to fabricate weft knitted fabrics. The PEDOT:PSS/PVA fibers survived repeated exposure to friction and tensile/bending strain in the knitting process without damage. MXene-coated PU fibers can be knitted into a single elbow sleeve by commercial-scale knitting machines for tracking various movements of the wearer's elbow in real time [101]. Both woven fabrics with vertical warp and weft yarns and knitted fabrics with crisscross loops can provide unique topographic clues for native anisotropic tissues [102,103]. Distributing conductive fibers in hydrogels or coating conductive fabrics with hydrogels can be seemed as feasible assembly methods for attenuating the interfacial problem between fiber assemblies and the targeted tissues, except that the isotropic hydrogel encapsulation will wipe off the structural feature of fiber assemblies especially anisotropy.

Textile technologies possess the advantages over other bio-fabrication technologies in controlling geometric structures, mechanical properties, pore structures and distribution of the loading molecules [104]. Besides, the processing parameters in this mature and controllable technology can be easily adjusted to achieve required properties.

3. Electrical signal transmitting for tissue repair

With the consensus on material-guided cell behaviors [105,106], great efforts have been put in geometrical cues (topographical structure) [107] and physical cues (mechanical, electrical, thermal and magnetic stimuli) transmitted by biomaterials [108]. Fiber manufacturing techniques offer unique advantages to construct biomimicking structures [34]. Moreover, with the involvement of conductivity into fibers, delivery of internal/external electrical signals can be facilitated for improving cell adhesion, differentiation, and proliferation for tissue

regeneration [100,105]. Hence, conductive fibers have been variously applied in regenerative medicine and tissue engineering for cardiac, nerves, bones and skins [109].

3.1. Cardiac tissue engineering

Myocardial ECM exhibits as an anisotropic, interwoven fibrous network that enables mechanical and electrical coupling between cardiomyocytes resulting in synchronous cardiac contraction [110,111]. After myocardial infarction (MI), the electroactive myocardium will be replaced by nonfunctional scar tissue, which inhibits coupled cellular communication [104]. Fortunately, the disconnected current path can be restored by a conductive patch attached to the myocardium, and the thinned ventricular wall, meanwhile, can be mechanically supported. Nevertheless, due to the lack of self-repair and renewal ability of the heart, CTE is expected to repair the heart by creating functional myocardium *in vitro* [112]. Cardiomyocytes rely heavily upon electrical signaling transmitted throughout the natural heart for tissue homeostasis and regular beating rhythms [113]. Hence, conductive fibers, in the form of cardiac patches and CTE scaffolds, have shown tremendous potentials in featuring biomimetic structural complexities [104].

3.1.1. Conductive cardiac patches

Upon being sutured or adhered to the epicardium, conductive cardiac patches are enabled to play the electrically restoring and mechanically supporting part for improving heart function after MI (Fig. 4A) [114–116].

An electrospun sub-micron fiber patch composed of shape memorable PU/PANI/silicon oxide (PU/PANI/SiO₂) was developed, which integrated 3D porous structure, specific thickness, elastic deformation, conductive stability, and self-adhesion property, and effectively reduced the infarction area after implantation [63]. The infarcted myocardium treated with aligned rGO/silk patches showed significant improvement on left ventricular (LV) pumping function including enhanced ejection fraction (EF), LV fractional shortening (LVFS), and ventricular fibrillation threshold compared with MI group [64]. Positive effect of the rGO/silk patch on alleviating the adverse myocardial remodeling was also displayed by preserving the LV wall thickness, reducing scar size and improving cardiomyocyte survival (Fig. 4B).

3.1.2. CTE scaffolds

CTE established upon 3D fibrous conductive scaffolds has become a potential strategy for regenerating heart tissues over the last decade [109,119]. The fibrous morphology of electrospun fiber mats mimics the structure of ECM, allows gas and nutrient exchange and provides directional guidance for cell alignment [120]. Compared to random CNT/silk scaffolds, aligned CNT/silk scaffolds were capable of promoting spreading and organization of cardiomyocytes, implicated by the improved formation of sarcomeres and gap junctions (Fig. 4C and D) [117]. Except for improved cell structure development (Fig. 4E and F), neonatal rat cardiomyocytes (NRCMs) cultured on PANi-contained fiber scaffold also exhibited favorable beating behaviors with longer contraction time, higher contractile amplitude, and lower beating rates [118]. PPy-encapsulated SF electrospun fiber mat was reported to enhance cardiac-specific protein expression, promote cell-cell couplings, and induce strong contractions [56]. The external electrical stimulus and the conductive fiber mat synergistically improved the cell alignment and contraction synchrony as well as increasing the beating frequency to 60 ± 8 bpm. These electrospun scaffolds coupling conductivity and fibrous structures may provide optimal stimuli to foster cell morphology and functions for myocardial regeneration or establishment of *in vitro* cardiomyocyte culture platform. A 3D printed-fibrous scaffold with controllable hexagonal microstructure was also prepared for myocardial regeneration [121]. And the *in vitro* studies confirmed the ability of the scaffold in promoting cell arrangement, sarcomere formation, and the expression of markers related with cardiac maturation.

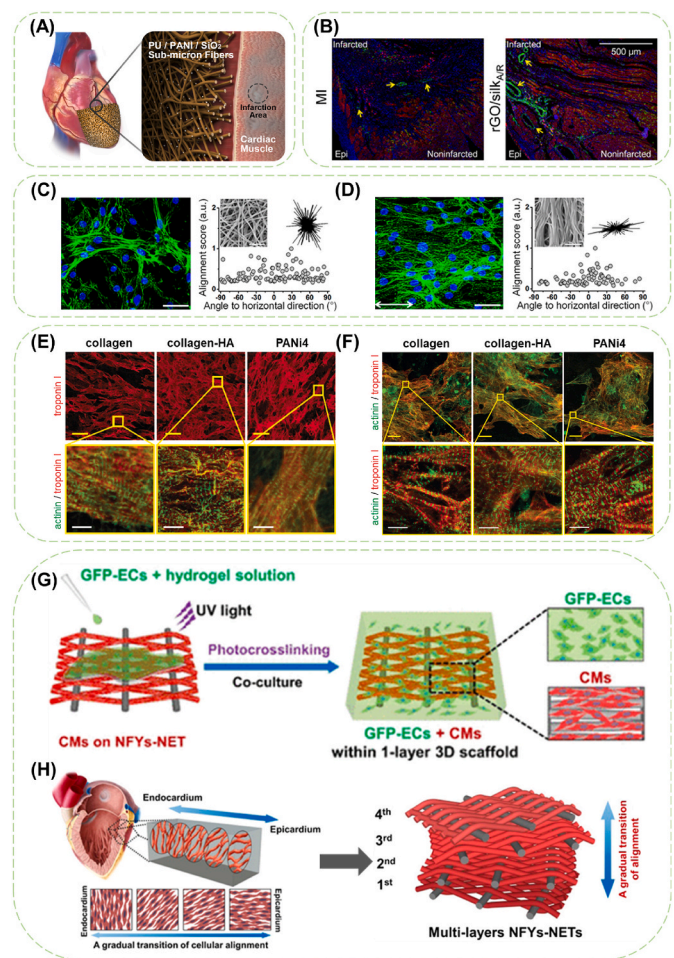


Fig. 4. The application of conductive fibers in cardiac patches and CTE scaffolds. (A) Representative treatment of a conductive sub-micron fiber cardiac patch to promote the electrical signal transduction. Reproduced with permission from Ref. [63] Copyright 2021, American Chemical Society. (B) Immunofluorescence images stained with cTnT and Cx-43 for the infarcted-noninfarcted transition areas. The yellow arrows indicate the microvascular structures stained by Cx-43. Reproduced with permission from Ref. [64] Copyright 2021, Acta Materialia Inc. F-actin staining images (scale bar: 20 μ m) and nucleus alignment analysis of cardiomyocytes on (C) random and (D) aligned CNT/silk fibrous scaffolds at day 7. Inset in the corner is the corresponding scanning electron microscope (SEM) image of the fibrous membrane (scale bar: 5 μ m). Reproduced with permission from Ref. [117] Copyright 2020, American Chemical Society. Confocal images of (E) NRCMs and (F) human induced pluripotent stem cells derived cardiomyocytes (hiPSC-CMs) cultured on electrospun fiber mats at day 5 stained for the cardiomyocyte-specific markers troponin I and/or sarcomeric- α -actinin. (Scale bars: (E): yellow: 25 μ m, white: 4 μ m; (F): yellow: 10 μ m, white: 4 μ m) Reproduced with permission from Ref. [118] Copyright 2019, The Authors. Creative Commons Attribution 4.0 International License. (G) Schematics showing the coculture procedure that cardiomyocytes were cultured on the NFYS-NET layer while green fluorescent protein-positive endothelial cells (GFP-ECs) were encapsulated within hydrogel shell. (H) Myocardium showing a gradual transition of aligned cell layers from endocardium to epicardium and schematics of multiple layers of fabrics assembled with the gradual transition of orientation. Reproduced with permission from Ref. [103] Copyright 2017, American Chemical Society.

Yarn and weaving technology have also been applied to the preparation of cardiac scaffolds. Wu et al. [103] fabricated a 3D hybrid scaffold based on nanofiber yarns network (NFYS-NET) layers within a photocurable methacrylated gelatin (GelMA) hydrogel shell to accommodate cardiomyocytes and endothelial cells (ECs). The NFYS-NET was woven with conductive nanofiber yarns as wefts and surgical sutures as

warps (Fig. 4G). The 3D hybrid scaffolds consisting of NFYs-NET layers were expected to induce aligned and elongated cardiomyocytes and to mimic the gradual transition of aligned cell layers from endocardium to epicardium (Fig. 4H), while the GelMA hydrogel shell were meant to provide a suitable 3D environment for mechanical protection and endothelialization. All the results showed the potential of conductive fabrics in myocardium regeneration.

3.2. Neural tissue engineering

Natural nerve tissue is composed of nerve bundles with multiple aligned assemblies, and transmits information mainly through action potential generated by synapses [122,123]. Hence, the orientation and electroconductivity of the matrix are of great benefits for guiding neuron alignment and transmission of electrical signals [124]. In results, conductive scaffolds and nerve conduits has shown remarkable effects in promoting nerve regeneration through cell proliferation and neural differentiation.

3.2.1. Conductive scaffolds

Geometry designs of nerve scaffolds have attracted serious attention due to the reports on electrical signals-assisted neural growth [125]. Composite fibrous scaffolds based on conductive materials and

biopolymers have been developed for promoting neurogenic differentiation of stem cells and cell behaviors of neurons [8,75,122,124].

Electrospun MWCNTs/PCL/gelatin nanofibers [8] were prepared to explore the synergistic effect of conductivity and fiber alignment on the differentiation of bone marrow mesenchymal stem cells (BMSCs) into Schwann cells (SCs). The BMSCs extended along the aligned fibers, while they distributed randomly on unoriented scaffolds as on the tissue culture plate. Moreover, the disparity in expression levels of S100 and GFAP indicated that the aligned nanofibers could promote the differentiation of BMSCs into SCs, and that the conductivity can further enhance the differentiation efficiency. Wu et al. [122] fabricated cell-laden PPy/collagen hydrogel microfibers with highly oriented microstructures to serve as nerve scaffolds. Cell spreading and elongating along the microfibers, formation of cell-cell contact networks, activation of voltage-gated calcium ion channels (crucial marker in early neurogenesis) were observed as well as enhanced expression of neurogenesis marker tubulin- β 3 and neurofilament protein. Additionally, the external electrical stimulation further promoted the neuronal functional expression. It shows the potential of conductive fiber scaffolds in constructing biomimetic microenvironment for neurogenesis. Wang's group [75] devised 3D conductive scaffolds with various microfiber patterns by NFES of poly (l-lactic acid-co-caprolactone) (PLCL), followed by GO coating of PLCL microfibers and *in situ* reduction of GO. The obtained

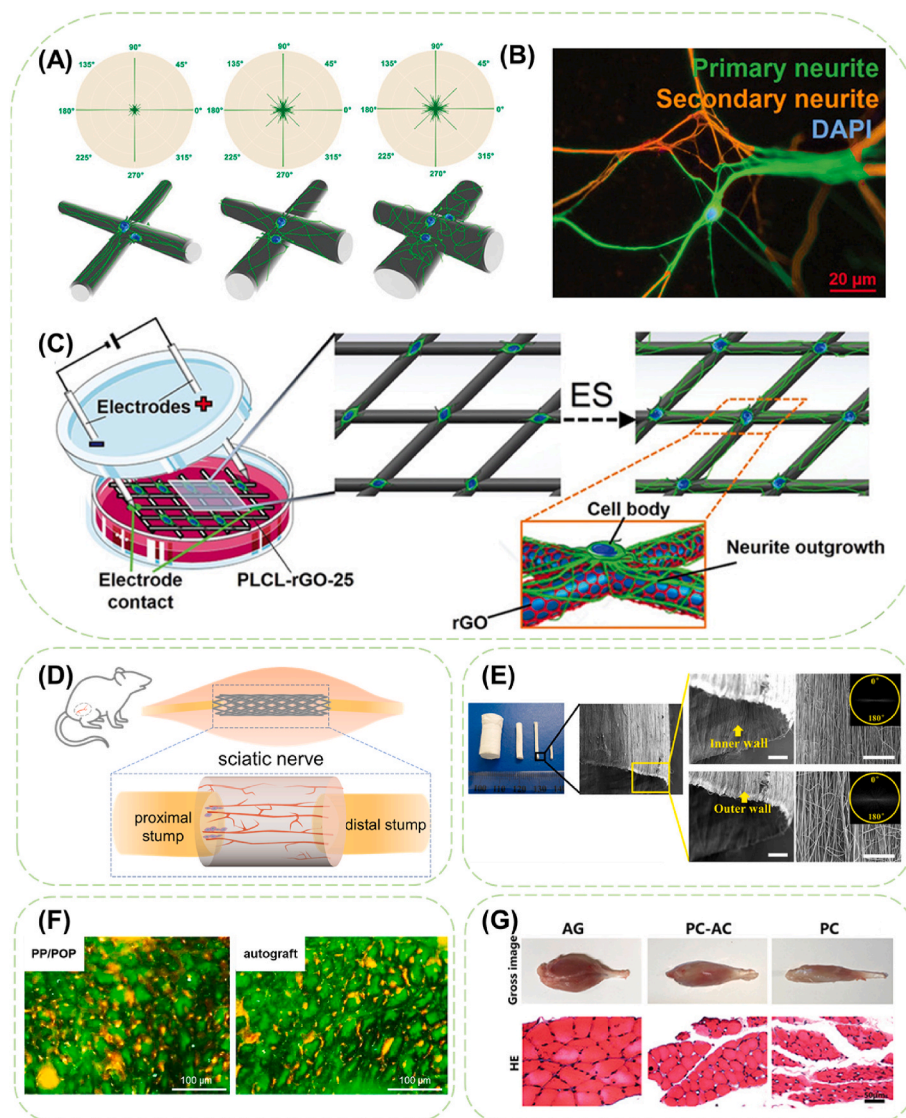


Fig. 5. The application of conductive fibers in nerve regeneration and repair. (A) Semi-quantitative analysis of the orientations of neurites of PC-12 cells on different diameter microfibers based on a python analysis. (B) Representative immunofluorescence image of the neurite outgrowth patterns, comprising primary (green) and secondary (orange) neurites, from a single PC-12 cell. (C) Schematic illustration of the culture setup with electrical stimulation to regulate the neurite outgrowth of PC-12 cells on rGO/PLCL conductive fiber scaffold. Reproduced with permission from Ref. [75] Copyright 2020, Wiley-VCH GmbH. (D) Schematic illustration of fibrous nerve conduit applied in rat sciatic nerve defect model. (E) Digital photo and SEM images of cellulose acetate butyrate nanofibrous conduits. (Scale bars: 100 μm) Reproduced with permission from Ref. [126]. Copyright 2015, American Chemical Society. (F) Immunofluorescence staining of the distal segments of the regenerated nerves repaired PP/POP conduits and autograft at 12 weeks post-operation. Reproduced with permission from Ref. [94]. Copyright 2018, Elsevier B.V. (G) Histomorphology and quantification of the gastrocnemius muscle in rats with sciatic nerve transection following nerve conduit implantation. HE staining showed the morphology of the myofibers of autograft (AG), PCL conduits containing aligned and conductivity nanofibers pre-seeded with BMSCs (PC-AC), and empty PCL conduits pre-seeded with BMSCs (PC) groups. Reproduced with permission from Ref. [8] Copyright 2020, The Authors. Creative Commons Attribution 4.0 International License.

scaffold with 25–50 layers of rGO exhibited superior conductivity ($\sim 0.95 \text{ S cm}^{-1}$) and capability of inducing neuronal-like network formation along the conductive microfibers under electrical stimulation (Fig. 5A–C). Overall, present studies have demonstrated that aligned conductive fibers play significant roles in cell differentiation and they can be used as a promising scaffold for nerve tissue engineering.

3.2.2. Nerve conduits

Apart from constructing engineered nerve tissue *in vitro*, nerve conduits stand for another approach especially applicable for treating nerve injuries over short distances ($< 4 \text{ cm}$) [127]. Proximal and distal nerve stumps are inserted into the two ends of the conduit, and axons start regenerating from the proximal end and gradually growing into the distal ends (Fig. 5D) [128]. Currently, nerve autografts remain as the most popular clinical approach for nerve reconstruction despite the disadvantages of insufficient tissue availability, mismatch in tissue size and structure, and donor site morbidity [129].

Conduits composed of well-arranged nanofibers have showed effectively promotion effect in sciatic nerve regeneration and thus been widely adopted in nerve conduit design (Fig. 5E) [126]. Jing et al. [94] developed a nerve conduit by filling PPy-coated aligned poly (lactic co glycolic acid) (PLGA) fibrous mesh into the lumen of the casted PPy/PLGA conduit (PP/POP) to verify the synergistic effects of combined stimuli of axially aligned fibers and conductive materials in nerve recovery. In comparison with rats treated with the non-conductive conduit or the non-filled conduit, the PP/POP-treated group showed significantly shorter latency period in compound muscle action potential (CMAP), higher peak CMAP value, and higher density of nerve axons, dictating raised nerve conduction velocity and better nerve regeneration.

Even though, such conductive nerve conduits are still inferior to autografts in terms of other recovery evaluations (Fig. 5F), which results in the involvement of biochemicals [130] and electrical stimulus. Scrolled CNTs/PCL composite fiber mat was combined with external pulsed current for neural repair [124]. Results of walking track analysis, electrophysiological analysis and H&E staining revealed that the oriented structure provided a favorable platform for remyelination and axonal regeneration and prevention of gastrocnemius muscle atrophy. Rat BMSCs were seeded on MWCNTs/PCL/gelatin nanofiber membranes and induced *in vitro* for 2 weeks, and then the membrane was rolled up and inserted into a PCL conduit [8]. The transplanted cells differentiated into mature SCs and participated in the formation of myelin sheath on MWCNTs-contained nanofibers. Furthermore, compared to PCL conduit, MWCNTs-contained conduit significantly improved the number of regenerated axons at middle and distal sites of the conduit, as well as the number of remyelinated axons at middle sites of the conduit, while showed no significant difference with the autograft. Moreover, the wet weight and myofiber area ratio of the gastrocnemius muscle treated with MWCNTs-contained conduit were considerably ameliorated, revealing the inhibitory action of myoatrophy after sciatic nerve injury (Fig. 5G).

3.3. Bone tissue engineering

Fibrous scaffolds have also been used for bone tissue repair due to their resemblance to native ECM and convenient fabrication [131]. In addition, enhanced osteogenic differentiation of stem cells under electrical stimulus aids to the growing applications of conductive scaffolds in bone tissue engineering [132,133].

The effects of scaffold porosity and conductivity on promoting osteogenic phenotype expression of osteoblast-like cells (MC3T3-E1) have been reported [134]. Yet, as scaffolds for bone tissue engineering, the structures, mechanical properties, biocompatibility and osteogenic bioactivity should be further improved. Electrospun GO/SF fibers showed ameliorated hydrophobicity and Young's modulus to support the growth and expansion of rat BMSCs [135]. The cytocompatibility and retention of exuberant cell proliferating effect of AuNPs/CNFs

scaffold were confirmed *via* both indirect and direct activity assay of osteosarcoma cells [136]. Current-induced substrates as cellulose nanocrystal/PCL electrospun fiber scaffold coated with GO [137], PANi-deposited PLLA nanofibrous film [138], 3D-printed CNT-encapsulated scaffolds [139] have been reported to enhance cell viability and osteogenesis. The PANi/PLLA scaffold exhibited good cell adhesion and cytocompatibility of BMSCs, and provided better promotion of cell proliferation, osteogenic differentiation and *in situ* biomineralization than that of the PLLA scaffolds [138]. The combination with water-soluble single-stranded deoxyribonucleic acid (ssDNA) presented a possible solution to the inherent cytotoxicity of CNT-based materials, and the homogenous distributed ssDNA@CNT nano-complex assisted excellent electrical field distribution surrounding the scaffold (Fig. 6A and B) [139]. Huang et al. [140] combined aligned MWCNTs, nano-hydroxyapatite and PCL by 3D printing to mimic the native fibrillar proteins and apatite in the human skeleton, in which cells spread on the filament surface indicated by extended and elongated actin filaments, and migrated and proliferated throughout the scaffold indicated by the well-distributed nuclei (Fig. 6C). Similarly, electrical microenvironment can be established by immobilization of PPy nanoparticles on the surface of PCL nanofibrous scaffolds, and enhanced calcium-phosphate crystal deposition was observed on the scaffold after electrical stimulation [141]. Moreover, the 3D printed-PCL/MWCNTs scaffolds could significantly promote angiogenesis and new bone formation with the assistant of electrical stimulation (Fig. 6D) [142]. The implanted scaffolds contribute to the recruitment of osteoclasts, and although the addition of MWCNTs seems to inhibit osteoclastogenesis, electrical stimulation appeared to be the dominant factor to promote osteoclast formation and functionality in the bone remodeling prevailing process. The complex and changeable combination of various fibers, metal ions, conductive polymers and ceramics shows great potential in the treatment of bone, cartilage and osteochondral defects.

3.4. Wound closure

Skin is another typical electroactive tissue where changes in epithelial potential indicates the destruction of skin structure caused by trauma, surgery, burns or chronic diseases [144]. Thus, conductive dressings and multifunctional sutures have been proposed and proven to accelerate wound healing through resetting the electrical field in the damaged area to restore, imitate or replace the function of the skin [145–148].

3.4.1. Wound dressings

Insufficient bioactivity and biodegradability of traditional wound dressings, as well as secondary injuries during replacement, would postpone the healing process. Hence, functional wound dressings with antibacterial activity, anti-inflammatory ability and proliferation promotion are strongly propelled.

Biocompatible and biodegradable SF is popular in wound dressings despite the demand of chemical modification against brittleness. PDA-assisted extraction process of silk fiber and deposition of PEDOT were combined to fabricate conductive silk-based microfibers (mSFs) [143]. PDA was adopted to protect the mSFs from excessive exposure to the corrosive alkaline solution, enhanced PEDOT assembling on the mSFs, and to promote the energy dissipation along the conductive mSFs, resulting in a good mechanical performance of the silk fiber-based patch embedded with the conductive mSFs. Owing to the combined effects of antioxidant PDA and conductive PEDOT, an accelerated healing process of diabetic wound was achieved (Fig. 6E), evidenced by the increased wound closed area, reduced epidermal gap and regenerated epidermal thickness, tight and uniform collagen deposition, reduced inflammatory response and controlled oxidative stress, all leading to the improved activity of fibroblasts and ECM reconstruction. Quaternized chitosan-graft-polyaniline (QCSP) modified PCL nanofiber membrane (PCL/QCSP) was fabricated to obtain a comprehensive performance of

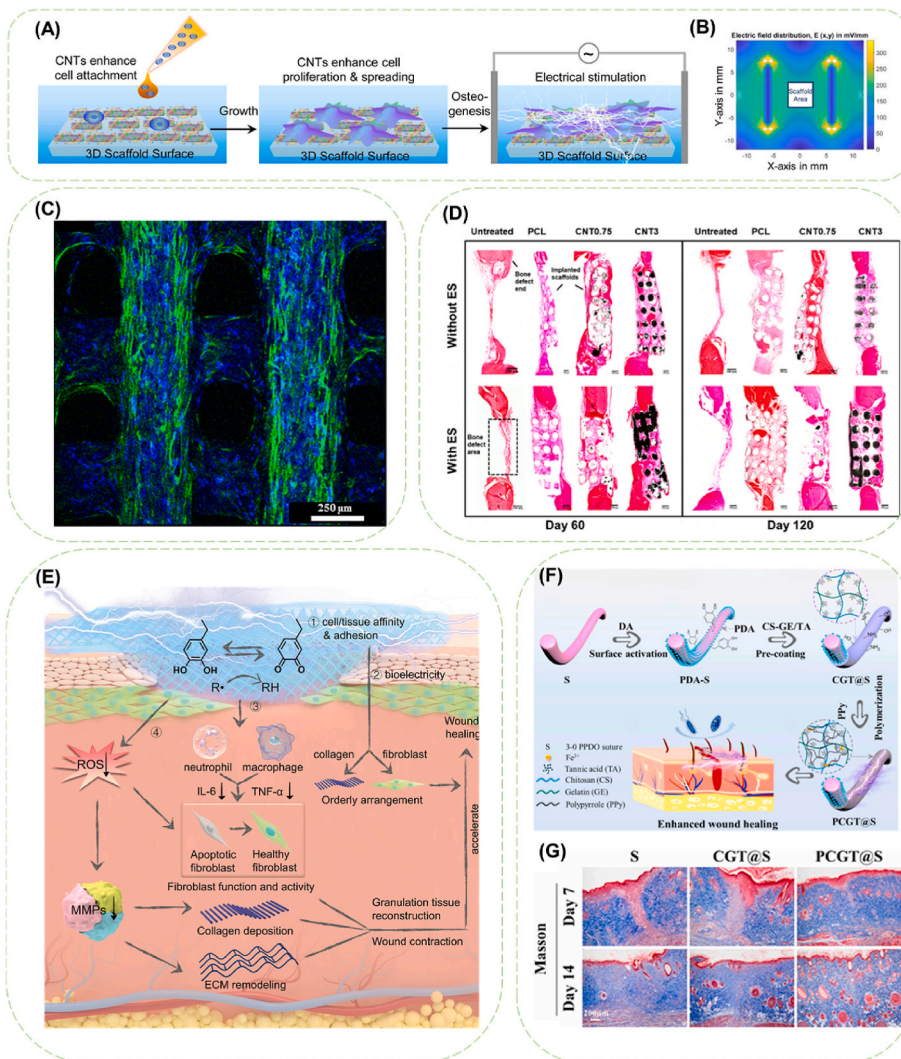


Fig. 6. Conductive fibers applied in bone tissue engineering and wound healing. (A) Schematic illustration of conductive scaffold guiding osteoblast growth and osteogenic differentiation of BMSCs in electrical microenvironment. (B) Electrical field distribution surrounding the scaffold area. Reproduced with permission from Ref. [139]. Copyright 2020, Acta Materialia Inc. (C) Confocal image showing cell distribution on the PCL/HA/MWCNTs scaffold. Reproduced with permission from Ref. [140]. Copyright 2019 Elsevier B.V. (D) The cross sections of bone tissue regeneration at the bone defect for PCL or PCL/MWCNTs scaffolds treated groups after 60 days and 120 days. Reproduced with permission from Ref. [142]. Copyright 2021, The Authors. Creative Commons Attribution 4.0 International License. (E) Schematic illustration of the mechanism of PEDOT-PDA-mSF patch in accelerated diabetic wound healing. 1) PDA promoted the cell adhesion and migration due to its cell/tissue affinity. (2) The conductive patch facilitated bioelectricity transmission. (3) The patch alleviated inflammation and (4) relieved oxidative stress. Reproduced with permission from Ref. [143]. Copyright 2021, Wiley-VCH GmbH. (F) Schematic fabrication process of the electroactive and antibacterial sutures. (G) The collagen deposition of PPDO suture (S), chitosan/gelatin/tannic acid coated-suture (CGT@S), and PCGT@S at day 7 and 14 post-operation. Reproduced with permission from Ref. [93]. Copyright 2021, Elsevier Ltd.

electroactivity, antioxidant and antibacterial ability for treating infection-susceptible chronic skin wounds [149]. The positively charged amino groups and quaternary ammonium groups in QCSP are effective for killing bacteria *via* electrostatic adherence. Consequently, PCL/QCSP showed better bacteria-killing behavior to *E. coli* compared to *S. aureus*, possibly because the down-regulated expression of genes vital to gram-negative bacteria occurs with the existence of PANi [150]. In the mouse full-thickness wounds defect model, after treatment with the PCL/QCSP, an ameliorated wound healing performance was confirmed by the enlarged wound contraction area, suppressed inflammatory cells infiltration, improved fibroblast immigration, regularized regenerated connective tissue and epithelium layer, increased thickness of granulation tissue, raised collagen deposition was observed all indicating ameliorated wound healing performance. Moreover, the immunohistochemical staining of vascular endothelial growth factor also revealed vascular angiogenesis which could further accelerate the wound healing process.

3.4.2. Conductive sutures

Sutures are common surgical instruments to facilitate wound closure by sealing the wound after incision or laceration. Nevertheless, lack of bioactivity and mismatched mechanical property of traditional sutures could result in delayed wound healing process and further cause acute wound failure or enlarged scar tissue.

With the as-mentioned promoting effect in wound healing,

functional conductive sutures have become another rising interest in wound healing [151–153]. Our research group constructed an electrically responsive and antibacterial suture (PCGT@S) with PPy *in situ* deposited on a polydioxanone suture pre-coated with chitosan/gelatin/tannic acid (CS-GE/TA) (Fig. 6F) [93]. The pre-coating of CS-GE/TA guarantees the adaptability between the brittle PPy and the flexible suture, and ensures the stable electrical signal conduction of PCGT@S even in knotted state. In addition, additive antibacterial effects of chitosan, tannic acid and PPy rendered a high bacteriostatic rate of 99%. Immunohistochemical results of PCGT@S treatment in the full-thickness skin defect showed obviously promoted skin wound healing and tissue regeneration (Fig. 6G).

In addition, raised tissue regeneration efficiency and continuously monitoring of suture integrity are of assistance to reduce wound failure and scar tissue formation. Therefore, efforts have also been devoted in electrically driven drug-eluting sutures and electronic sutures sensing physiological variations of wound sites. Lee and coworkers [152] developed a drug release electronic suture system (DRESS) to monitor suture integrity in real time and to achieve on-demand drug release. The DRESS was composed of a AgNPs-embedded PU multifilament core and a drug-containing thermosensitive polymer shell. The conductive core plays a role of a highly sensitive and mechanical durable strain sensor while the thermoresponsive shell promotes the on-demand drug release by Joule heating under a 130 mV-voltage. Stable mechanical property, resistive response and temperature response were maintained when

repeated stretch-release cycles were applied to the DRESS-sutured injured porcine skin. Moreover, monitoring the physicochemical states of deep surgical sites post-operatively is necessary to prevent infection, dehiscence and other complications. Wireless sensing (WiSe) sutures were prepared by PEDOT:PSS-functionalized silk sutures encapsulated in biocompatible parylene-C [153]. Functioning as a dipole antenna, the WiSe suture can be assembled with an electronic pledget consisting of a Schottky diode, a capacitive sensor and a tuning inductor, and this completes the construct of a wireless sensing system. The wireless sensing system enables transducing changes due to infection or leakage in the deep surgical site into shifts in the resonant dip of the harmonic signal spectrum. Monitoring of the wound integrity, gastric leakage and tissue fretting in porcine and the healing outcomes in rat model comparable to medical-grade sutures showed the ability of battery-free wireless detection of post-surgical complications and wound closure.

4. Conductive fibers in implantable bioelectronics

Next generation of implantable or wearable bioelectronics for single-point health monitoring requires the introduction of new features including flexibility, large area and facile processing of 1D or 2D materials, controlled biological properties, and mixed electronic and ionic conductivity [154], which just right falls into the advantages of textile technology and fiber materials. Therefore, conductive fiber-based implantable devices including signal capture devices, biosensors and implantable supercapacitors have been widely studied.

4.1. Biopotential acquiring electrodes

Electroencephalogram, electrocardiograph, and electromyography

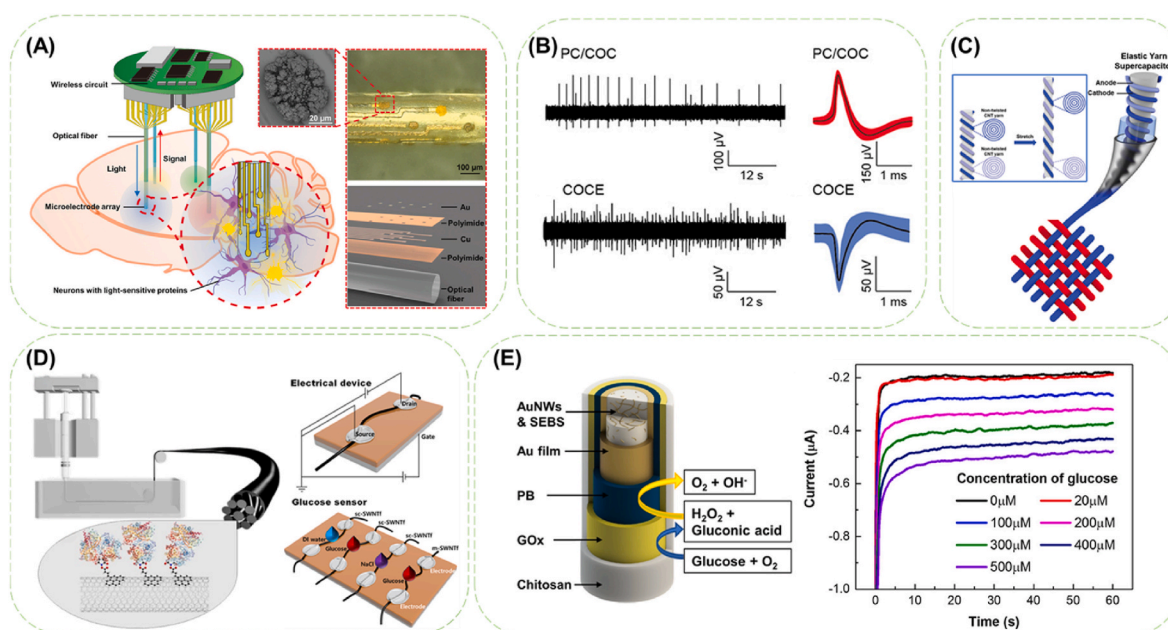


Fig. 7. Conductive fibers acting as a component in implantable bioelectronics. (A) Schematic of the device implanted into different areas of the rat brain. An image and an exploded view (right) of a flexible optoelectronic fiber that consists of an optical fiber and eight microelectrodes whose surface has been coated with AuNPs (inset). Reproduced with permission from Ref. [158]. Copyright 2021, Wiley-VCH GmbH. (B) Spontaneous activity recorded in acute conditions with AgNW concentric mesh electrodes deposited onto two different core fibers (PC/COC: cyclic olefin copolymer (COC) wrapped-polycarbonate fiber; COCE: thermally drawn-COC elastomer fiber) in mice spinal cord and corresponding action potentials isolated from the recording. Reproduced with permission from Ref. [162]. Copyright 2017, The Authors. Creative Commons Attribution 4.0 International License. (C) Scheme and principle of supercapacitor based on CNT yarn twist. Supercapacitor consists of two non-twisted CNT yarns for anode and cathode. When stretching the supercapacitor, both non-twisted CNT yarns are constant. Reproduced with permission from Ref. [164]. Copyright 2020, WILEY-VCH Verlag GmbH & Co. KGaA, Weinheim. (D) Wet spinning of separated SWCNTs and enzyme immobilization, and characterizations of m- and sc-SWCNT fibers (gate effect and glucose sensing). Reproduced with permission from Ref. [165]. Copyright 2020, The Authors. Creative Commons Attribution 4.0 International License. (E) Schematic illustration of the fiber working electrode and the chronoamperometric responses of the fiber-based glucose sensor to the increasing glucose concentrations from 0 to 500 μM. Reproduced with permission from Ref. [84]. Copyright 2019, American Chemical Society.

the diffusion of water molecules and the relaxation of polymer chains in aqueous environment. Real time neuronal signal recording and single unit neuronal signal recording were achieved due to the same size of CNT fiber as neuron after the implantation of the dry MFNP into the cerebral cortex of adult mice. Besides an outperforming SNR (>5), stable electrochemical performance and limited inflammatory response ensured stable neural recording for 4 weeks post implantation. Conductive fiber is also composable with optoelectronic probes for realizing simultaneously electrophysiological recording and optical neuromodulation of spinal cord. The resilient concentric electrode composed of AgNWs mesh-deposited elastomer fibers can maintain low impedance at strain up to $\sim 100\%$ and record spontaneous neural activity and sensory-evoked potentials after implantation (Fig. 7B) [162]. As a composite electrode, the aligned CNF deposited with alternate Au and Ag nano layers had a significantly decreased impedance and could maintain a relatively stable impedance at 1 kHz [163]. The integrated nanostructured electrode arrays provided continuous electrophysiology measurements up to 28 weeks post-implantation without concerning tissue response.

Besides signal acquisition, conductive fibers can also be used as temporary pacing wires for correcting abnormal heart rates. Zhou et al. [166] attempted to improve the existing carbon-fiber-based temporary transvenous cardiac pacing metal leads by using carbon-fiber-graphene-woven leads or conductive cloth. The results showed that the carbon fiber bundle was stable and easily deformed under lower stress to reduce the damage to the myocardium, which demonstrates excellent clinical application value. Hang et al. [167] proposed an absorbable temporary epicardial pacing wire (TPW) based on screen-printed EGaIn circuits on PLCL membranes. The as-prepared TPW displayed excellent conductivity, flexibility, cycling stability (>100000 cycles), minor inflammatory response and 13% degradation during two-month subcutaneous implantation, avoiding secondary injuries of removal surgery and migration of the remaining wires.

4.2. Fiber-based supercapacitors

For implantable electronic devices, supercapacitors appear to be more ideal as power supply due to their high energy and power density, high capacity, and long life cycle, as long as the issues of conventional supercapacitors including rigidity, heavy weight, unstable electrolytes and degradation are solved [168]. Fiber-based supercapacitors are characterized by lightweight, flexibility, bendability, braidability and scalability [169].

Conductive fibers are enabled to integrate the electrodes and insulation layer of supercapacitors by partial modification on the fiber. Region-specific reduction of GO fiber enabled integrating rGO layer as electrodes with GO fiber as the separator into one single fiber to function as a flexible fiber supercapacitor without extra bonding agent or assembly process [170]. CNT yarns insulated by PU coating were wound around a pre-stretched rubber mandrel and packed in a silicone rubber tube, which was assembled as an elastic yarn supercapacitor after injecting solid electrolyte into the rubber tube (Fig. 7C) [164]. The elastic yarn supercapacitor exhibited a constant capacitance (capacitance change $<3\%$) within 70% strain and a stable electrochemical storage capacity with dynamic sinusoidal stretching of 70% and 180° bending deformation during 1000 cycles. Although the electrolyte was separated from outer environment, the limited wettability of CNTs to the typical hydrophilic electrolyte always led to a relatively low energy density in CNT-based supercapacitors.

In order to resolve the biotoxicity issue of electrode materials, bio-modification on electrodes emerges as possible strategies to evade the influence on cell activity. Kim's group dip-coated MWCNTs with biocompatible PEDOT:PSS/ferritin nanoclusters and fabricated PEDOT:PSS/ferritin/MWCNTs (PFM) fiber supercapacitor by a bi-scrolling process [171]. Capacitance of the PFM supercapacitor was enhanced by the support of PEDOT:PSS for charge transport between ferritin and

MWCNTs, and by the increased loading of high capacitance-PEDOT:PSS on MWCNTs through reducing electrostatic repulsion. Meanwhile, the PFM fiber showed 90% remained capacitance eight days after stitched in mouse abdominal muscle and minimized restriction on motion besides good biocompatibility.

The leak issue of electrolytes in fiber supercapacitors brings challenges in electrolyte encapsulation and is partially conquered by utilizing body fluid directly as an electrolyte. The supercapacitor formed by hydrophilic aligned CNTs fibers twisting into a double-helix, was able to work in physiological fluid with an enhanced energy storage capability due to the high pseudocapacitance introduced by the oxygen-containing groups [172]. Without additional packaging, the specific capacitance of the CNT fiber supercapacitor reached 11.4 F/g and 13 F/g in serum and blood, respectively, as well as a stable specific capacitance after 10000 cycles in phosphate buffered saline (PBS). Jang et al. [173] reported an implantable CNT yarn supercapacitor based on the redox system of Nicotinamide adenine dinucleotide (NAD) in living cells. The CNT yarn electrodes exhibited a maximum area capacitance (55.73 mF/cm^2) in PBS and serum, and a negligible loss of capacitance after 10000 repeated charge/discharge cycles and bending/knotting deformation. More importantly, the CNT yarn electrodes implanted into the abdominal cavity of a rat skin revealed a stable electrical performance *in vivo*.

It is highly desirable to design and fabricate biodegradable energy storage devices with high energy/power densities and long cycling life for implanted bioelectronics. The most straightforward and feasible strategy is to utilize a series and parallel connection to construct energy storage devices arrays, which require biodegradable/bioabsorbable conducting wires [174]. Another promising strategy is to construct battery-supercapacitor hybrid system made of a high-capacity battery electrode and a high-rate capacitive electrode [175]. Besides *in vivo* applications, conductive fibers-based supercapacitors can also be used in intelligent wearable electronic devices [176–179] which is more mature in fabrication due to lower requirements in flexibility, size and biocompatibility and resultingly not covered in this review.

4.3. Biosensors

Early detection and continuous monitoring of disease markers play a key role in disease diagnosis and treatment. Conductive fibers have also emerged as a possible strategy to improve the performance of biosensor devices.

The use of carbon nanomaterials, metallic nanoparticles, nano-structured conductive polymers and MXenes as electroactive medium has improved the performance of bio/chemical sensors. Co_3O_4 nanoparticles-doped carbon nanofibers prepared by electrospinning and carbonization combined high electrochemical conductivity and good biocompatibility and synergistically enhanced the immobilization of redox protein [180]. MWCNTs-functionalized electrospun nanofibers were reported as electrodes in an electrochemical sensor to detect the neurotransmitter dopamine, whose abnormal level is associated with various diseases such as schizophrenia and Parkinson's disease [181]. The as-prepared electrode displayed a limit of detection (LOD) of 0.15 $\mu\text{mol/L}$ within the linear range of 1–70 $\mu\text{mol/L}$ despite existence of interfering molecules. However, 82% remaining of the initial current value after 100 cycles indicated the insufficient stability. CNT fibers twisted into helical bundles showed bending stiffness close to soft tissue and injectability, enabling spatially resolved and real-time monitoring of H_2O_2 when implanted in mice tumours, and monitoring Ca^{2+} and glucose in cat's venous blood *in vivo* when integrated with a wireless transmission system [182]. PEDOT-embedded electrospun rubber nanofiber pre-attached with ssDNA probe sequence achieved electrochemical sensing of non-Hodgkin lymphoma gene with an ultra-low LOD of 1 aM ($1 \times 10^{-18} \text{ mol/L}$) [183]. The 400-fold improvement in LOD compared to a thin-film sensor analogue was realized by the improved hydrophilicity and high surface area brought by electrochemically polymerization of functionalized EDOT and sequentially

grafting of poly (acrylic acid) brushes on the fibers surface. Such specific gene sensor helps to develop quick, accurate “liquid biopsies” for early disease detection meanwhile avoiding tissue biopsies.

Enzyme immobilization on conductive fibers is also adopted to achieve accurate sensing of biomolecules. Purified SWCNTs were wet spun into microfibers followed by glucose oxidase fixation as biosensor platform for glucose (Fig. 7D) [165]. Gold-sputtered PCL nanofibrous membranes exhibited higher sensitivity of hydrogen peroxide detection compared to similar Au layer-deposited Si/SiO₂ wafers due to their higher surface area [184]. Upon immobilizing of superoxide dismutase by chemically crosslinked cysteine, the PCL/Au fiber presented a sensitivity of 16.1 $\mu\text{A mM}^{-1} \text{cm}^{-2}$, a LOD of 1.9 μM detecting H₂O₂ and recoverable determination of superoxide in cell culture media. Different methods of enzyme immobilization affect the electron transfer process between the fibers and the enzyme active site and the encapsulation amount of enzymes, thus limiting the saturation levels upon enzyme immobilization and availability. Hence, new-generation biosensors are requiring enzyme-free biosensing for low-cost and easy fabrication.

In addition to biocompatibility, biodegradability is also considered in biosensors for both immunity and operation concerns. Wet-spun PEDOT:PSS fiber was coated with optically transparent, photocrosslinkable SF sheath for insulation and protection, and the obtained core-sheath fiber worked as a fully organic and free-standing flexible biosensor of ascorbic acid which can be proteolytically biodegraded in a few weeks [185]. On the other hand, noninvasive wearable electrochemical biosensors built upon conductive fiber-based three-electrode systems have also drawn great attention for sensing electrophysiological and biochemical signals, or delivering drugs, which are very useful for patients in detecting diseases at an early stage. Stretchable Au/SEBS fiber sequentially modified with Prussian blue, glucose enzyme and chitosan to complete the design of fiber working electrode, which demonstrated clear and quantitative response with a sensitivity of 11.7 $\mu\text{A mM}^{-1} \text{cm}^{-2}$ toward glucose in the range of glucose level in the sweat (from 0 to 500 μM) (Fig. 7E) [84]. Along with reduced requirement in biocompatibility comes with the leveled-up requirement in conformability, air permeability and stretchability between the fiber-based bioelectronics and the wearing site and the cycling performance of wearable fiber-based bioelectronics under frequented deformation.

5. Conductive fibers in wearable bioelectronics

The distinguished characteristics of fiber-based conductive materials over thermoplastic polymers, thermosetting polymers or hydrogels as wearable bioelectronics are usually manifested as their durability and wearing comfortability. The former originates from mechanically compliance and resistance to friction and washing, while the latter bases

on flexibility as in recoverable folding, bending, stretching, and compressing deformations and breathability resulting from appropriate heat and moisture management. Typical applications of conductive fibers in wearable bioelectronics are categorized as conductors, electrical resistors for electrothermal therapy, and strain/pressure sensors for monitoring pulses, breaths and blood pressure.

5.1. Stretchable conductors

For wearable electronic devices, stretchability is indispensable for proper functioning during inevitable limb activity (Table 1). Researchers first focused on improving the elasticity of conductive fibers, mostly through compositing with elastomers commonly seen in the form of conductive coating on elastic fibers. However, the poor interaction and the huge differences in mechanical properties between elastomers and conductive coatings require the participation of soft adhesives to fix conductive components as well as avoid instant mechanical failure. A conductive fiber with a 500% elasticity formed by EGaIn coating on PU fiber via the hydrogen bonds from the intermediate polymethacrylate (PMA) layer, which can serve as a stable conductor for ECG electrodes when stretched to 100% [186]. Unfortunately, owing to the smooth and less elastic outer conductive layer, the conductivity of the fiber still showed an inevitable 40% decrease when stretched from 0% to 500%.

The pre-stretching method can easily improve the strain-insensitive performance of conductive fibers besides their tensile elongation. The strain-insensitive range and the quality factor (QF, defined as the percentage of strain divided by the percentage of resistance change) of CNT/SEBS core-sheath fibers can be further enlarged by overcoating a SEBS layer outside the CNT layer to reduce the contact between CNT buckles under low strain, and even further by winding the buckled fiber into coils [98]. Worm-shaped graphene/PU fiber could attain a strain-insensitive range up to 220% [97].

Despite these achieved elongation rates, along with large strain deformations always comes a reduction in conductivity, and the working strain range of conductive fiber still needs to be determined according to different applications. Inspired by the structure of the electroactive muscle fiber bundles, our group designed an ultrastretchable (>1000%) conductive multifilament with buckled PPy structure in parallel, which showed an excellent recoverability within 100% strain, and a small hysteresis within 200% strain [82]. Due to the flexible PPy doped with plasticizer and the paralleled buckles, the current paths in the multifilament were able to be stabilized even at 900% tensile strain (Fig. 8A). While the coaxial wet-spun TPE/PEDOT:PSS fiber pre-stretched to 900% can be reversibly stretched up to 680% with less than 4% change in resistance, when applied in LED lightning and joule heating, it can only endure a 520% strain and a 400% strain respectively for stable current

Table 1
Conductive fibers applied as stretchable conductors.

components	structure	Conductivity (S cm ⁻¹)	breaking strain	maximum operating strain	QF	cycling performance
PU@PMA@EGaIn [186]	smooth core-sheath fiber	>10 ³	~600%	523%	N/A	8000; 40% (8000 cycles under 40% strain)
PU@(Graphene/PU) [97]	worm-shaped buckled fiber	1.24	1010%	815%	11.26	4000; 10%
PU@PDA@PPy [82]	buckled filaments in parallel	2.38	>1000%	>900%	10.9	1500; 20%
(PEDOT:PSS/PBP)@TPE [38]	buckled ribbons in channels	~90	~675%	500%	~193	1800; 300%
(PU/Cu)@cyanoacrylate [83]	3D helical fiber	>10 ⁴	~400%	300%	N/A	10000; 30%
SEBS@CNT fiber [98]	buckled core-sheath fiber	~18	1350%	1000%	~222	N/A
EGaIn/fluoroelastomer [187]	smooth core-sheath fiber	4.35 × 10 ⁴	1170%	650%	50	600; 100%
Au/fluorine rubber [99]	wrinkled fiber mat	~10 ¹	1000%	170%	0.75	500 cycles each under 30% and 60% strain respectively

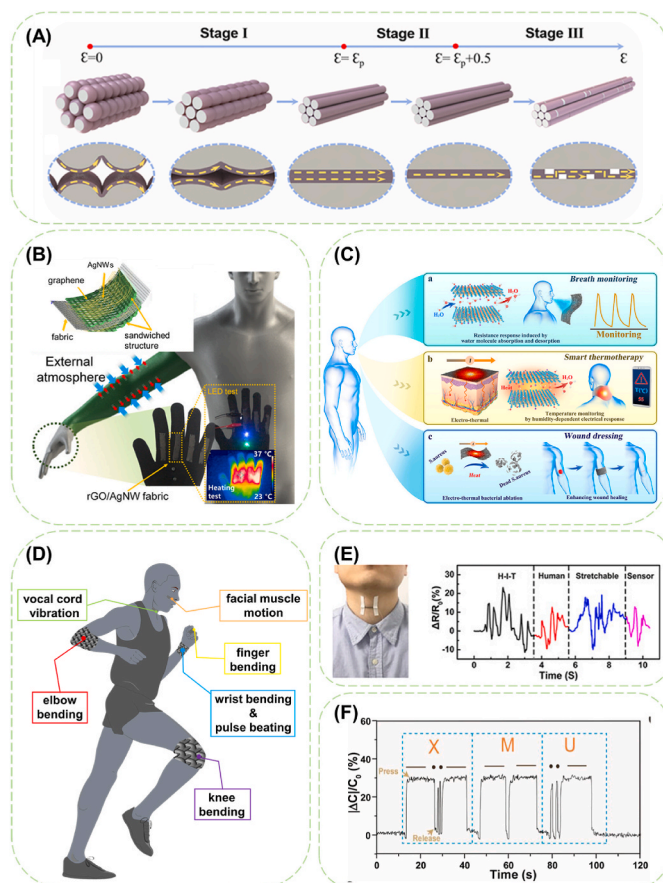


Fig. 8. Flexible conductive fibers acting as stretchable conductors, heaters and physical sensors in wearable health devices. (A) Working mechanism of the parallel conductive multifilament and current path (yellow arrow) along the multifilament under increasing strain. Reproduced with permission from Ref. [82]. Copyright 2022, The Authors. Creative Commons Attribution 4.0 International License. (B) Wearable rGO/AgNW fabric as a thermal sensor. Reproduced with permission from Ref. [188]. Copyright 2021, American Chemical Society. (C) Conceptual illustration of flexible and wearable MXene-based smart fabrics. Reproduced with permission from Ref. [189]. Copyright 2020, American Chemical Society. (D) Schematic illustration of fiber-based strain sensors for body motion monitoring. (E) Photograph of the second strain sensor attached to the throat and relative resistance changes of the second strain sensor when the wearer spoke H-I-T, human, stretchable, and sensor. Reproduced with permission from Ref. [190]. Copyright 2019, American Chemical Society. (F) Signal output for the Morse code “XMU” when the intelligent glove with pressure sensor was knocking the corresponding codes. Reproduced with permission from Ref. [191]. Copyright 2019, WILEY-VCH Verlag GmbH & Co. KGaA, Weinheim.

[38]. The 3D helix PU/Cu fibers prepared with 400% pre-strain showed extremely soft behavior before reaching the limiting strain of approximately 200%, but its working range should be set within 100% strain considering resistance change [83].

Residual plastic deformation after pre-strain limits the actual working range below the pre-strain amplitude, which means only the large reversible mechanical deformation can improve practical tensile performance. Based on the unconventional positive piezoconductivity effect of LM-embedded elastomers brought by stretch-induced elongation of LM particles [38,192], Zheng et al. [187] utilized the dipole-dipole interactions between fluoroelastomer and LM to prepare a highly stretchable, leakless and conductance-stable EGaIn-based core-sheath microfiber through coaxial liquid wet spinning and “freezing-plus-stretching”-induced activation of conductive path. The prepared microfiber showed stable conductance under stretching,

compressing, twisting, and bending primarily contributed by the stretching out of the original highly tortuous serpentine conductive path. Still, preservation of the high conductance of liquid metal requires rupture of the initially resistive oxidation layer on LM particles and isolation from the atmosphere, which is difficult to ensure in wearable bioelectronics.

Although some cyclic performance issue still exists, with the enriched structure designs in conductive fibers, stable electrical connection for the functional device in the circuit of wearable bioelectronics can be ensured.

5.2. Joule heaters for personal thermal management

Thermal therapy has attracted vital attention with its practical and effective action in personal thermal management and pain-relieving physiotherapy for rheumatic arthritis rehabilitation, muscle spasms, and inflammation alleviation, reducing joint stiffness and improving blood circulation and collagen tissue flexibility [193–196].

Conductive fibers are well-suited for fabricating devices for body heat management by converting electrical energy to thermal energy in a more convenient and unconstrained way. The stretchable conductors also showed potentials as wearable heaters since nearby thermal field comes along with migration of charged carriers in the conductors. 2 cm-long TPE/PEDOT:PSS fiber can generate a temperature of 42 °C at 6 V under up to 200% strain [38]. However, the applied voltage is higher than the desired value of wearable heaters and the temperature window is not wide enough for different thermal management usage scenarios.

For wearable heaters, low-voltage driving, high thermal conversion efficiency and durability are necessary for safety, feasibility and practicability. EGaIn-based core-sheath microfiber with a high conductivity of $\sim 10^4$ S cm⁻¹ showed a voltage-relevant heating behavior (from 25.5 °C at 0.2 V to 71.9 °C at 1.2 V), and a great cyclic heating performance of 40 heating-cooling cycles with short temperature switching period (6.5 s for heating and 9 s for cooling) [187]. The photothermal effect of MXene can also be utilized to realize a tunable temperature variation and high thermal conversion efficiency [197]. The wrinkled thermoplastic polyurethane (TPU)/MXene fiber mat showed a steady surface temperature of 81 °C under up to 50% strain at 4 V and uniform temperature distribution on bended finger [198]. Durability for wearable heaters demands abrasive resistance, washing fastness, stable flexibility and resistance after cyclic deformation. Park et al. [95] fabricated a shape-adaptable fiber heater by coating MXene on amine-functionalized polyester (PET) threads, without delamination of MXene flakes or significant resistance changes after 100 bending cycles at a bending angle of 60°.

Arrangement of conductive fibers through weaving/knitting/braiding process is used to construct electrical heating element in designated positions on the fabrics more precisely. Cheng et al. [199] fabricated a woven heating fabric with Cu nanowire-based composite fibers for fabricating heating kneepad for articular thermotherapy. Compared to the fabrics with conductive coating, weaving of conductive fibers can maximumly preserve air permeability while achieving a uniform and stable conductivity. Large-area thermal homogeneity is significant for wearable heaters in addition to thermal stability [200], which requires stable heating performance of conductive fibers after being assembled into fabrics. Besides, high-resolution site-specific heating is also beneficial for disease-related local thermal therapy [201].

The urge to miniaturize electronics for wearable health monitoring devices drives multicomponent integration, multi-functionalization and intellectualization. The supersonically sprayed rGO and AgNWs coating layer on the nylon/PU fabric could offer hydrophobicity, wearability, stretchability, washability, mechanical durability, and antibacterial features, so the composite fabric can form a multi-functional device as heater, supercapacitor, and strain/temperature monitor (Fig. 8B) [188]. Zhao et al. [189] constructed a platform for mobile healthcare and personal medical therapy based on MXene-deposited nonwoven

cellulose fabric, which enables respiration monitoring, electrothermal therapy with real-time temperature monitoring and warning, Joule heating-induced sweat/moisture evaporation and bacterial ablation integratively (Fig. 8C). Stable electrothermal performance was displayed by a maintained highest temperature of 45 °C at a voltage of 3 V during 20 on-off cycles, and slight resistance change after 1000 bending/recovery cycles.

Despite all the efforts in developing stretchable Joule heaters, expectations like low-voltage powering, programmable temperature control process and cyclic heating performance after repeated forces have not been completely received. This calls for development of an all-in-one wearable platform achieving both general and symptom-specific electrothermal therapy for body temperature management in harsh weather condition and for disease-related heat unbalance.

5.3. Strain/pressure sensors for body motion monitoring

Human-machine interfaces (HMI) demand recognition of the motion states or physiological function states of the applied body sites to execute set instructions. The conformability and electrical response of conductive fibers can be utilized to realize accurately mechanical sensing on the deformable human body (Fig. 7D). Mechanical deformations always result in geometries changes such as stretching, separation, and microcracking within the matrix of the conductive fibers, thus leading to relevant variations in conductive paths [202–204]. Therefore, when the quantitative relations between the electrical resistance/voltage/capacitance and the external mechanical forces are determined, real-time monitoring of body motion can be decided (Table 2).

5.3.1. Fiber/yarn-based strain/pressure sensors

Conventional strain sensors fabricated from rigid materials are too

Table 2
Conductive fiber and fabrics applied as strain/stress sensors.

sensor type	substrates	conductive components	conductivity	sensitivity	range	response and recovery time (ms)	
resistive sensor	fiber/yarn-shaped strain sensor	PU multifilament [186]	EGaIn	10^3 S cm^{-1}	GF = 1.5	0–500%; 0.1–2 Hz	220; 280
		EVA fiber [205]	CNT	$\sim 0.026 \text{ S cm}^{-1}$	GF = 3.25 GF = 33.29	0–88% 88–190%	312; 327 N/A
		TPE fiber [204]	CNT	93.145 S cm^{-1}	GF = 21.3 GF = 34.22	0–150% 200–1135%	16; N/A N/A
		PU fiber [206]	AgNW/MXene	$\sim 266 \Omega \text{ cm}^{-1}$	GF > 100	0–100%	344; 344
		wet spun recycled cellulose fiber [37]	PANi	17.3 mS cm^{-1}	GF = 23.8	2.5–5%	N/A
		microfluidic spun natural rubber fiber [51]	CNT/PEDOT:PSS	$19.1 \text{ k}\Omega \text{ cm}^{-1}$	GF = 3.66–4.4	0–1275%	63; N/A
		Spandex yarn [207]	$\text{Ti}_3\text{C}_2\text{T}_x$	$105 \text{ k}\Omega \text{ cm}^{-1}$	GF = 604.0 GF = 1.2×10^4 GF = 5.7×10^4	0.11–36.6% 36.6–55.6% 55.6–61.2%	N/A
fiber/yarn-shaped pressure sensor	twisted nylon yarn [208]	CuNPs	$1200 \Omega \text{ cm}^{-1}$	0.57 kPa^{-1}	0.01–200 kPa	2; 2	
		CNT/ $\text{Ti}_3\text{C}_2\text{T}_x$ /AuNPs	47.72 S cm^{-1}	0.94 kPa^{-1}	0–20 kPa	39; N/A	
		carbon black nanoparticles	$34.6 \text{ k}\Omega$	GF = 62.2	0–30%	40; 270	
		PPy	N/A	GF = 3.8 GF = 5.9 GF = 38.9	0–200% 0–125% 0–65%	N/A	
		GO/carbon fiber	N/A	GF = 49.8 GF = 830.7	0–45% 45–50%	300; 300 N/A	
fabric-shaped pressure sensor	microfluidic spun PAN fiber membrane [46]	graphene nanoplatelets/carbon black	$\sim 1.95 \text{ k}\Omega$	GF = 1.67 GF = 6.05	0–120% 120–150%	N/A N/A	
		CNT/ $\text{Ti}_3\text{C}_2\text{T}_x$	$6.6 \pm 1.5 \Omega/\square$	0.245 kPa^{-1} 0.060 kPa^{-1}	0.128–1.9 kPa 1.9–12.9 kPa	N/A	
	nonwoven cotton fabric [212]	$\text{Ti}_3\text{C}_2\text{T}_x$	134.2Ω	5.30 kPa^{-1} 2.27 kPa^{-1} 0.57 kPa^{-1}	0–1.30 kPa 1.30–10.25 kPa 10.25–40.73 kPa	N/A	
			N/A	0.08 kPa^{-1} 3.844 kPa^{-1} 12.095 2.27 kPa^{-1} 0.57 kPa^{-1}	40.73–160 kPa 0–29 kPa 29–40 kPa 1.30–10.25 kPa 10.25–40.73 kPa	50; 20 N/A 26; N/A N/A	
			N/A	0.08 kPa^{-1}	40.73–160 kPa	50; 20	
	cotton fabric [214]	$\text{Ti}_3\text{C}_2\text{T}_x$	N/A	GF = 0.7 GF = 0.91 N/A GF = 12 N/A	0–30% 0–950% 0–15% 15–27.5% 27.5–50%	N/A 180; N/A N/A	
			440 S cm^{-1}	GF = 6.02 GF = 2.3×10^6	2.8–19.7% 0–100%	N/A 170; 170	
N/A			N/A	100–250%	N/A		
N/A			GF = 1.55	0–15%	N/A		
capacitive sensor	melt-spun Hytrel fiber [215]	carbon black	N/A	GF = 0.7	0–30%	N/A	
		CNT	$26.1 \Omega \text{ cm}^{-1}$	GF = 0.91	0–950%	180; N/A	
		AgNPs	N/A	N/A	0–15%	N/A	
	cellulose yarns [217]	$\text{Ti}_3\text{C}_2\text{T}_x$	N/A	GF = 12 N/A	15–27.5% 27.5–50%	N/A	
			440 S cm^{-1}	GF = 6.02 GF = 2.3×10^6	2.8–19.7% 0–100%	N/A 170; 170	
wet spun TPU fiber [218]	CNT	N/A	N/A	100–250%	N/A		
nylon/spandex weft-knitted fabric [209]	carbon black nanoparticles	N/A	N/A	GF = 1.55	0–15%	N/A	

bulky and inflexible to be applied in wearable purposes. Joint motions of fingers, wrists, elbows, knees and necks usually have large, low frequency bending strains up to 55% [219], while the minor motions of pulses, heartbeats, vocal cord (Fig. 8E), hand gesture (Fig. 8F) and muscles relevant to facial expression have smaller, high frequency tensile/compression strains as low as 0.1% [190,191,205]. Flexible conductive fibers consequently emerge to realize multidimensional reversible strain while retaining desired sensing performance.

Typical textile-based resistive strain sensors fabricated by coating/dispersing conductive components on/in elastomers have the simplest structure design. A strain sensor for detecting the bending motion of knee joints was constructed through sewing PEDOT:PSS-coated PET yarns linearly on woven fabrics with insulated PET yarns, while a physically disconnected space left between two conductive yarns on the fabrics was further employed to forming a touch sensor [220]. Similarly, EGaIn/PMA/PU fiber can be used to prepare a strain sensor to detect the bending of fingers, wrists, elbows and knees, separately [186]. Despite the easy assembly, these sensors usually suffer from poor stretchability and poor cycle performance.

Designs in fiber structures are reasonably employed to improve sensor performance. Elastic multifilament is selected as substrates for flexible sensors due to their high stretchability and specific surface area. The GF value of the AgNPs/PU multifilament could reach up to $\sim 9.3 \times 10^5$ under a large strain within 300–450%, which was used to monitor the large volume expansion of artificial bladder system [221]. Though, both slow tensile deformation and the permanent slippery/disentanglement of the unstrained filaments will cause inevitable electrical and mechanical hysteresis after the loading-unloading cycles. Winding structures of core-spun yarns, twisted yarns and helical fibers are highly beneficial for improving tensile performance. Core-spun yarns with CNT-coated cotton fiber sheath and PU filament core showed a stable cycling performance of nearly 300,000 times under 40% strain [222]. The relative current change of the PU/cotton/CNT yarn stayed stable after the 40,000th cycling test and was recognizable under 10% strain at 4–15 Hz frequencies, which is completely satisfied the request of detecting minor muscle motions. Strong adhesion of CNT on degummed silk fibers allowed twisted CNT/silk yarns (CSYs) enduring automatic machinability and washing [201]. Gloves sewed with CSYs exhibited stable electrical responses during 200 bending-releasing cycles and potential in recognizing and digitalizing hand gestures. Intertwined core-sheath EGaIn/elastomer fiber was adopted to form a double helix-structured multifunctional capacitive sensor [223], which performed indistinguishable torsion sensing range between -10° and 25° , a lowest detection limit at 2.90%, and rapid recognition of finger tapping. Moreover, the buckling structure of conductive coatings can broaden the working range of strain sensors. Buckled CNT/TPE fiber strain sensor reached a stretchability up to 1135% [204]. The sensor enabled simulating a Parkinson's tremor through characteristic waveforms of resistance changes, and detecting both subtle muscle movements and large deformation of the cervical vertebra through values of resistance changes. Besides, potential in real-time quantitative assessment of tendon rehabilitation was also demonstrated by attaching the sensor as an implantable device to rat tendon and recording the angle of the tibia in the relaxed state and stretching state.

Apart from resistive sensors, conductive fibers are also constructed into capacitive sensors with competitiveness on linearity, hysteresis and response time despite at the cost of low sensitivity ($GF \leq 1$) [224]. Lee et al. [216] designed a highly sensitive passive wireless fiber strain-sensing system with a hollow double helical structure formed by AgNPs/PU multifilament and insulated with PDMS coating, and an antenna coil fabricated by AgNPs/PU multifilament was directly connected to the sensor through the transmission line. By implanting it into an *ex vivo* and *in vivo* porcine leg model, the potentials in continuously monitoring biomechanical strain of an Achilles tendon during movements were well displayed. Moreover, with CNTs acting as bridges across the cracks generated between AgNPs, hollow-porous

CNT/AgNPs/TPU sensing fiber with an ultra-high GF of 2.3×10^6 was prepared, which could detect both subtle and vigorous human movements like breathing and squatting [218].

5.3.2. Fabric-based strain/pressure sensors

Textiles possess inimitable advantages of good breathability, tailorability, and excellent mechanical compliance to conformably attaching to the human body. Textile technologies including weaving, knitting, braiding and embroidery can be fully used to fabricate conductive fabrics for physical sensors.

Coating conductive biomaterials on intact fabrics is a facile approach for fabricating wearable sensors. The thick and porous structure of conductive fabrics grant sufficient free volume and elasticity allowing for continuous changes in contact area sensitive to body strain. MXene-coated cotton fabrics reached a wide linear range of 0–140 kPa and effective detection of simulated static tremor of the early stage of Parkinson's disease with a frequency of 6 Hz while showing a decreasing trend in the sensitivity with increasing applied pressure [213]. In consideration of the typical interface delamination issue, a topographical modification technique was developed to enable strong adhesion of nickel particles on polyacrylamide-modified cotton fabrics [203]. The as-prepared fabric electrodes formed a parallel capacitor with a minimum measurable distance and bending angle of 19 μm and 0.05° , respectively, which can be applied to evaluate training effects of rehabilitation by monitoring the contraction of abdominal muscles at standing, sitting, and lying states. Due to the strong tendency of stacking up of conductive nanosheets [225], fabric sensors based on graphene/MXenes still suffer from limited sensitivity and detection range, which may be ameliorated by microstructures constructing of the fabric coatings despite at a higher cost [212,214].

Weaving and knitting manifest as a more creative technique for obtaining balanced sensing performance. PPy/PVA-dip coated fabric handwoven by polyester yarns and rubber bands into different structures showed a structure-dependent sensitivity and sensing range [210]. Upon being integrated with a wireless transmitter, real-time monitoring of subtle muscle motion as vibrations of vocal cords and frowning, and large muscle motion as bending of wrist, elbow, and knee joint, can be remotely received and displayed on a smartphone. Loop structured fabric knitted by double-helix yarns gained superior free volume and elasticity, which realized a balanced performance on sensitivity (0.57 kPa^{-1}), response time (2 ms), relaxation time (2 ms), linearity (4.9%), variation (7.8%), durability (6000 cycles), and hysteresis (5.3%) [208]. The knitted fabric can be applied in precise pulse monitoring and analysis of radial artery and carotid artery, which can ultimately diagnose vascular aging by evaluating the condition of arterial stiffness, and potentially realizing the unique pulse taking and palpation in traditional Chinese medicine. Moreover, the mechanical properties and distribution of the conductive component in the fabrics can be adjusted by fabric structures. Despite the slightly reduced flexibility, MXene-coated cellulose yarns were able to be subjected to knitting machines and to be knitted into different loop structures with different stitch patterns [217]. Half-gauge and interlock stitch patterns increased the space between each line of the loops and reduced the yarn-to-yarn friction and yarn breakage. A capacitive strain sensor was constituted by knitting MXene-coated bamboo yarns into interlock stitch pattern with a thin nitrile rubber insulation, which showed constant capacitive response during 2000 compressing-relaxing cycles and was capable of distinguishing various pressure levels of applied finger touching.

On top of these strain/pressure sensors, electrical responses to other physical stimulus including temperature, humidity and solvents can be comprehensively utilized into recognition of complex condition around the applied body interface. Detecting and identifying external stimulus of stretching, heating and humidifying was realized through different responses of resistance and capacitance of the carbon black nanoparticles-deposited nylon/spandex knitted fabric [209]. Normally, the increased resistance and decreased capacitance correspond to

stretching, while the exactly contrary changes correspond to heat and the increase in both resistance and capacitance corresponds to humidity. A multifunctional sensor based on CSY with water repellency and organic solvent resistance was developed, displaying the ability of detecting ethanol concentrations in aqueous ethanol solutions in addition to temperature and external forces [201].

Despite the excellent performance of the as-stated sensors displayed in labs, it is necessary for these novel conductive fiber-based materials to focus on the issue of stiffness, flexibility, conductivity stability and cyclic performance under high-frequency repetitive strain, friction and washing, to achieve a unification of wide linear range, high sensitivity and low hysteresis in a real use scenario, and conquer the issue of instability facing varying conditions including unusual temperature, humidity, and solvent [226].

6. Conclusions and future prospects

Conductive fibers and fibrous constructs with all sorts of geometry structures and properties have been successfully fabricated by blending spinning and surface modification on fibers, consequently meeting the application-specific requirements due to variable applied sites and aimed functions in the biomedical field. On the one hand, wet spinning, microfluidic spinning, electrospinning and 3D printing of mixture of fiber-forming polymers and conductive components are facile methods to balance the mechanical property and conductivity of the fibers and less likely to cause conductivity loss due to interface exfoliation. On the other hand, surface modification is convenient to be combined with stretching, winding and/or fixing process to construct buckled, helical or serpentine conductive fibers with improved mechanical properties to endure large and repeated deformations under body motion and organ function. Nevertheless, such conductive fibers still lack solutions of high-throughput, simplified, and low-cost fabrication strategy, which hinders the mass production and clinical translation. The convergence of conventional textile technologies and precision machining can be a competitive future direction for addressing this particular issue.

Based on the consensus on the positive influence of conductivity to electroactive tissues, fibrous conductive scaffolds have been widely used in promoting tissue repair and regeneration progress. Conductive fibers with tissue-specific structure and property designs have showed the regulation role of electrical signals in cell behaviors, including orientation, ultrastructure development, and cellular organization of neurons and cardiomyocytes, and migration, proliferation and recruiting of osteoblasts and fibroblasts. In order to recapitulate the original microenvironment of electroactive tissues, researchers have shed light on constructing three-dimensional multiscale heterogeneous scaffolds with ECM-mimicking feature by conductive fibers for researches on tissue repair of nerve, myocardium, bone and skins. Electrically responsive drug delivery system can also be built upon conductive fibrous scaffolds and integrated with implantable biosensors and stimulator to realize intelligent personalized disease therapy. Despite these positive effect in tissue repair and regeneration, clinical translation of conductive fibers is still hindered due to the problematic long-term fatigue behavior against the sophisticated service demand in physiological environment. Furthermore, despite the unclarified biophysical and biochemical mechanism behind exogenous electrical stimulation on cells, the combination of conductive fibrous scaffolds and electrical stimulation benefits directed differentiation of stem cells and functional maturation of stem cell-derived cells. Moreover, despite the blooming bioprinting technology and cell coculture technique, it remains as a huge challenge to propose a cell-compatible precursor formula of conductive fibers to achieve tissue engineered constructs by one-step fabrication.

In addition to being transmitted among cells or across tissues, the endogenous electrical signals can also be acquired and analyzed directly by probing electroactive tissues or indirectly by conversion from mechanical/biochemical signals related to organ functions, which is beneficial to reflect human health state in time. This calls for quick

development for implantable and wearable bioelectronics. However, the repeated and large deformation and yet minor electrical changes put forward strict requirements on the mechanical and electrical properties of the materials used in the implantable and wearable bioelectronics, which is exactly the reason that conductive fibers received extensive attention in this field. Accurate and timely signal transduction and transformation demand tight contact and synchronous deformation between the contacting surface of the device and the applied body site, as well as reasonable structure designs of components and superior conductivity, especially for the wearable devices aimed to be applied on the joint parts. Meanwhile, for the implantable devices, the main challenges are microminiaturization and long-term biocompatibility, which requires detectivity up to cellular level, simplicity of implanting method and degradability/simplicity of removal method. Besides, multifunctionalization and battery-free and wireless operation are becoming the major trend in developing bioelectronics. This requires the integration of electronic devices and consequently calls for thorough designs in the structure and performance of conductive fibers. In clinical practice.

Declaration of competing interest

The authors declare that they have no known competing financial interests or personal relationships that could have appeared to influence the work reported in this paper.

Acknowledgments

The authors acknowledge the support from the National Natural Science Foundation of China (Grant No. 52005097), the Natural Science Foundation of Shanghai (Grant No. 21ZR1401300), the Fundamental Research Funds for the Central Universities (2232022A-05), the Fundamental Research Funds for the Central Universities and Graduate Student Innovation Fund of Donghua University (CUSF-DH-D-2021022), the 111 Project (Grant No. BP0719035), and the Fundamental Research Funds for DHU Distinguished Young Professor Program.

References

- [1] M. Levin, C.G. Stevenson, Regulation of cell behavior and tissue patterning by bioelectrical signals: challenges and opportunities for biomedical engineering, *Annu. Rev. Biomed. Eng.* 14 (2012) 295–323.
- [2] S. He, J. Wu, S.H. Li, L. Wang, Y. Sun, J. Xie, D. Ramnath, R.D. Weisel, T.M. Yau, H.W. Sung, R.K. Li, The conductive function of biopolymer corrects myocardial scar conduction blockage and resynchronizes contraction to prevent heart failure, *Biomaterials* 258 (2020), 120285.
- [3] S. Yoshida, K. Sumomozawa, K. Nagamine, M. Nishizawa, Hydrogel microchambers integrated with organic electrodes for efficient electrical stimulation of human ipsc-derived cardiomyocytes, *Macromol. Biosci.* 19 (6) (2019), 1900060.
- [4] C. Song, X. Zhang, L. Wang, F. Wen, K. Xu, W. Xiong, C. Li, B. Li, Q. Wang, M.M. Q. Xing, X. Qiu, An injectable conductive three-dimensional elastic network by tangled surgical-suture spring for heart repair, *ACS Nano* 13 (12) (2019) 14122–14137.
- [5] M.D. McCauley, F. Vitale, J.S. Yan, C.C. Young, B. Greet, M. Orecchioni, S. Perike, A. Elgalad, J.A. Coco, M. John, D.A. Taylor, L.C. Sampaio, L.G. Delogu, M. Razavi, M. Pasquali, In vivo restoration of myocardial conduction with carbon nanotube fibers, *Circulation: Arrhythmia. Electrophysiol.* 12 (8) (2019), e007256.
- [6] L. Du, T. Li, F. Jin, Y. Wang, R. Li, J. Zheng, T. Wang, Z.-Q. Feng, Design of high conductive and piezoelectric poly (3,4-ethylenedioxythiophene)/chitosan nanofibers for enhancing cellular electrical stimulation, *J. Colloid Interface Sci.* 559 (2020) 65–75.
- [7] E. Tomaskovic-Crook, P. Zhang, A. Ahtiainen, H. Kaisvuo, C.Y. Lee, S. Beirne, Z. Aqrave, D. Svirskis, J. Hyttinen, G.G. Wallace, J. Trivas-Sejdic, J.M. Crook, Human neural tissues from neural stem cells using conductive biogel and printed polymer microelectrode arrays for 3D electrical stimulation, *Adv. Healthc. Mater.* 8 (15) (2019), 1900425.
- [8] X. Hu, X. Wang, Y. Xu, L. Li, J. Liu, Y. He, Y. Zou, L. Yu, X. Qiu, J. Guo, Electric conductivity on aligned nanofibers facilitates the transdifferentiation of mesenchymal stem cells into Schwann cells and regeneration of injured peripheral nerve, *Adv. Healthc. Mater.* 9 (11) (2020), 1901570.

- [9] X. Dai, B.C. Heng, Y. Bai, F. You, X. Sun, Y. Li, Z. Tang, M. Xu, X. Zhang, X. Deng, Restoration of electrical microenvironment enhances bone regeneration under diabetic conditions by modulating macrophage polarization, *Bioact. Mater.* 6 (7) (2021) 2029–2038.
- [10] J. Yang, Y. Xiao, Z. Tang, Z. Luo, D. Li, Q. Wang, X. Zhang, The negatively charged microenvironment of collagen hydrogels regulates the chondrogenic differentiation of bone marrow mesenchymal stem cells in vitro and in vivo, *J. Mater. Chem. B* 8 (21) (2020) 4680–4693.
- [11] S. Lee, B. Ozlu, T. Eom, D.C. Martin, B.S. Shim, Electrically conducting polymers for bio-interfacing electronics: from neural and cardiac interfaces to bone and artificial tissue biomaterials, *Biosens. Bioelectron.* 170 (2020), 112620.
- [12] R. Das, E.J. Curry, T.T. Le, G. Awale, Y. Liu, S. Li, J. Contreras, C. Bednarz, J. Millender, X. Xin, D. Rowe, S. Emadi, K.W.H. Lo, T.D. Nguyen, Biodegradable nanofiber bone-tissue scaffold as remotely-controlled and self-powering electrical stimulator, *Nano Energy* 76 (2020), 105028.
- [13] Y. Liang, X. Zhao, T. Hu, B. Chen, Z. Yin, P.X. Ma, B. Guo, Adhesive hemostatic conducting injectable composite hydrogels with sustained drug release and photothermal antibacterial activity to promote full-thickness skin regeneration during wound healing, *Small* 15 (12) (2019), 1900046.
- [14] R. Yu, H. Zhang, B. Guo, Conductive biomaterials as bioactive wound dressing for wound healing and skin tissue engineering, *Nano-Micro Lett.* 14 (1) (2021) 1.
- [15] R. Luo, J. Dai, J. Zhang, Z. Li, Accelerated skin wound healing by electrical stimulation, *Adv. Healthc. Mater.* 10 (16) (2021), 2100557.
- [16] B.W. Walker, R.P. Lara, E. Mogadam, C.H. Yu, W. Kimball, N. Annabi, Rational design of microfabricated electroconductive hydrogels for biomedical applications, *Prog. Polym. Sci.* 92 (2019) 135–157.
- [17] A. Mariano, C. Lubrano, U. Bruno, C. Ausilio, N.B. Dinger, F. Santoro, Advances in cell-conductive polymer biointerfaces and role of the plasma membrane, *Chem. Rev.* 122 (4) (2022) 4552–4580.
- [18] Y. Yu, H.Y.Y. Nyein, W. Gao, A. Javey, Flexible electrochemical bioelectronics: the rise of in situ bioanalysis, *Adv. Mater.* 32 (15) (2020), e1902083.
- [19] B. Llerena Zambrano, A.F. Renz, T. Ruff, S. Lienemann, K. Tybrandt, J. Vörös, J. Lee, Soft electronics based on stretchable and conductive nanocomposites for biomedical applications, *Adv. Healthc. Mater.* 10 (3) (2021), 2001397.
- [20] S. Peng, Y. Yu, S. Wu, C.-H. Wang, Conductive polymer nanocomposites for stretchable electronics: material selection, design, and applications, *ACS Appl. Mater. Interfaces* 13 (37) (2021) 43831–43854.
- [21] E.N. Zare, T. Agarwal, A. Zarepour, F. Pinelli, A. Zarrabi, F. Rossi, M. Ashrafzadeh, A. Maleki, M.-A. Shahbazi, T.K. Maiti, R.S. Varma, F.R. Tay, M. R. Hamblin, V. Mattoli, P. Makvandi, Electroconductive multi-functional polypyrrole composites for biomedical applications, *Appl. Mater. Today* 24 (2021), 101117.
- [22] C.O. Baker, X. Huang, W. Nelson, R.B. Kaner, Polyaniline nanofibers: broadening applications for conducting polymers, *Chem. Soc. Rev.* 46 (5) (2017) 1510–1525.
- [23] H. Luo, Y.V. Kaneti, Y. Ai, Y. Wu, F. Wei, J. Fu, J. Cheng, C. Jing, B. Yuliarto, M. Eguchi, J. Na, Y. Yamauchi, S. Liu, Nanoarchitected porous conducting polymers: from controlled synthesis to advanced applications, *Adv. Mater.* 33 (29) (2021), 2007318.
- [24] M.C. Serrano, M.C. Gutiérrez, F. del Monte, Role of polymers in the design of 3D carbon nanotube-based scaffolds for biomedical applications, *Prog. Polym. Sci.* 39 (7) (2014) 1448–1471.
- [25] M.A. Deshmukh, J.-Y. Jeon, T.-J. Ha, Carbon nanotubes: an effective platform for biomedical electronics, *Biosens. Bioelectron.* 150 (2020), 111919.
- [26] M.D. Dozois, L.C. Bahlmann, Y. Zilberman, X. Tang, Carbon nanomaterial-enhanced scaffolds for the creation of cardiac tissue constructs: a new frontier in cardiac tissue engineering, *Carbon* 120 (2017) 338–349.
- [27] S.R. Shin, Y.C. Li, H.L. Jang, P. Khoshkhalagh, M. Akbari, A. Nasajpour, Y. S. Zhang, A. Tamayol, A. Khademhosseini, Graphene-based materials for tissue engineering, *Adv. Drug Deliv. Rev.* 105 (Pt B) (2016) 255–274.
- [28] S. Talebian, M. Mehrali, R. Raad, F. Safaei, J. Xi, Z. Liu, J. Foroughi, Electrically conducting hydrogel graphene nanocomposite biofibers for biomedical applications, *Front. Chem.* 8 (2020) 88.
- [29] J. Yan, Y. Lu, G. Chen, M. Yang, Z. Gu, Advances in liquid metals for biomedical applications, *Chem. Soc. Rev.* 47 (8) (2018) 2518–2533.
- [30] Y.G. Park, G.Y. Lee, J. Jang, S.M. Yun, E. Kim, J.U. Park, Liquid metal-based soft electronics for wearable healthcare, *Adv. Healthc. Mater.* 10 (17) (2021), 2002280.
- [31] R. Feiner, T. Dvir, Tissue–electronics interfaces: from implantable devices to engineered tissues, *Nat. Rev. Mater.* 3 (1) (2017), 17076.
- [32] R. Chen, A. Canales, P. Anikeeva, Neural recording and modulation technologies, *Nat. Rev. Mater.* 2 (2) (2017), 16093.
- [33] J. Lee, B.L. Zambrano, J. Woo, K. Yoon, T. Lee, Recent advances in 1D stretchable electrodes and devices for textile and wearable electronics: materials, fabrications, and applications, *Adv. Mater.* 32 (5) (2020), 1902532.
- [34] M. Akbari, A. Tamayol, S. Bagherifard, L. Serex, P. Mostafalu, N. Faramarzi, M. H. Mohammadi, A. Khademhosseini, Textile technologies and tissue engineering: a path toward organ weaving, *Adv. Healthc. Mater.* 5 (7) (2016) 751–766.
- [35] X.-X. Wang, G.-F. Yu, J. Zhang, M. Yu, S. Ramakrishna, Y.-Z. Long, Conductive polymer ultrafine fibers via electrospinning: preparation, physical properties and applications, *Prog. Mater. Sci.* 115 (2021), 100704.
- [36] L. Lan, C. Jiang, Y. Yao, J. Ping, Y. Ying, A stretchable and conductive fiber for multifunctional sensing and energy harvesting, *Nano Energy* 84 (2021), 105954.
- [37] C. Wang, Y. Li, H.Y. Yu, S.Y.H. Abdalkarim, J. Zhou, J. Yao, L. Zhang, Continuous meter-scale wet-spinning of cornlike composite fibers for eco-friendly multifunctional electronics, *ACS Appl. Mater. Interfaces* 13 (34) (2021) 40953–40963.
- [38] J. Zhou, G. Tian, G. Jin, Y. Xin, R. Tao, G. Lubineau, Buckled conductive polymer ribbons in elastomer channels as stretchable fiber conductor, *Adv. Funct. Mater.* 30 (5) (2019), 1907316.
- [39] Y. Dong, L. Wang, J. Wang, S. Wang, Y. Wang, D. Jin, P. Chen, W. Du, L. Zhang, B.-F. Liu, Graphene-based helical micromotors constructed by “microscale liquid rope-coil effect” with microfluidics, *ACS Nano* 14 (12) (2020) 16600–16613.
- [40] Y. Yu, J. Guo, B. Ma, D. Zhang, Y. Zhao, Liquid metal-integrated ultra-elastic conductive microfibers from microfluidics for wearable electronics, *Sci. Bull.* 65 (20) (2020) 1752–1759.
- [41] S. Pan, P. Wang, P. Liu, T. Wu, Y. Liu, J. Ma, H. Lu, Stable cellulose/graphene inks mediated by an inorganic base for the fabrication of conductive fibers, *J. Mater. Chem. C* 9 (17) (2021) 5779–5788.
- [42] Q. Gao, M. Wang, X. Kang, C. Zhu, M. Ge, Continuous wet-spinning of flexible and water-stable conductive PEDOT: PSS/PVA composite fibers for wearable sensors, *Compos. Commun.* 17 (2020) 134–140.
- [43] Q. Gao, P. Wang, M. Wang, Y. Wang, J. Zhu, Metal salt modified PEDOT: PSS fibers with enhanced elongation and electroconductivity for wearable e-textiles, *Compos. Commun.* 25 (2021), 100700.
- [44] X.Y. Du, Q. Li, G. Wu, S. Chen, Multifunctional micro/nanoscale fibers based on microfluidic spinning technology, *Adv. Mater.* 31 (52) (2019), 1903733.
- [45] Q. Zhao, H. Cui, Y. Wang, X. Du, Microfluidic platforms toward rational material fabrication for biomedical applications, *Small* 16 (9) (2020), 1903798.
- [46] Y. Wu, T. Yan, K. Zhang, Z. Pan, Flexible and anisotropic strain sensors based on highly aligned carbon fiber membrane for exercise monitoring, *Adv. Mater. Technol.* 6 (12) (2021), 2100643.
- [47] J. Jiao, F. Wang, J.-J. Huang, J.-J. Huang, Z.-A. Li, Y. Kong, Z.-J. Zhang, Microfluidic hollow fiber with improved stiffness repairs peripheral nerve injury through non-invasive electromagnetic induction and controlled release of NGF, *Chem. Eng. J.* 426 (2021), 131826.
- [48] Y. Yu, F. Fu, L. Shang, Y. Cheng, Z. Gu, Y. Zhao, Bioinspired helical microfibers from microfluidics, *Adv. Mater.* 29 (18) (2017), 1605765.
- [49] W. Ma, D. Liu, S. Ling, J. Zhang, Z. Chen, Y. Lu, J. Xu, High-throughput and controllable fabrication of helical microfibers by hydrodynamically focusing flow, *ACS Appl. Mater. Interfaces* 13 (49) (2021) 59392–59399.
- [50] Q.W. Cai, X.J. Ju, S.Y. Zhang, Z.H. Chen, J.Q. Hu, L.P. Zhang, R. Xie, W. Wang, Z. Liu, L.Y. Chu, Controllable fabrication of functional microhelices with droplet microfluidics, *ACS Appl. Mater. Interfaces* 11 (49) (2019) 46241–46250.
- [51] T.N. Lam, G.S. Lee, B. Kim, H. Dinh Xuan, D. Kim, S.I. Yoo, J. Yoon, Microfluidic preparation of highly stretchable natural rubber microfiber containing CNT/PEDOT:PSS hybrid for fabric-sewable wearable strain sensor, *Compos. Sci. Technol.* 210 (2021), 108811.
- [52] F. Daneshvar, S. Tagliaferri, H. Chen, T. Zhang, C. Liu, H.-J. Sue, Ultralong electrospun copper-carbon nanotube composite fibers for transparent conductive electrodes with high operational stability, *ACS Appl. Electro. Mater.* 2 (9) (2020) 2692–2698.
- [53] B. Zhang, F. Kang, J.-M. Tarascon, J.-K. Kim, Recent advances in electrospun carbon nanofibers and their application in electrochemical energy storage, *Prog. Mater. Sci.* 76 (2016) 319–380.
- [54] Y. Zhang, G.C. Rutledge, Electrical conductivity of electrospun polyaniline and polyaniline-blend fibers and mats, *Macromolecules* 45 (10) (2012) 4238–4246.
- [55] B. Guo, P.X. Ma, Conducting polymers for tissue engineering, *Biomacromolecules* 19 (6) (2018) 1764–1782.
- [56] Y. Liang, A. Mitriashkin, T.T. Lim, J.C.-H. Goh, Conductive polypyrrole-encapsulated silk fibroin fibers for cardiac tissue engineering, *Biomaterials* 276 (2021), 121008.
- [57] H. Nazari, S. Azadi, S. Hatamie, M.S. Zomorrod, K. Ashtari, M. Soleimani, S. Hosseinzadeh, Fabrication of graphene-silver/polyurethane nanofibrous scaffolds for cardiac tissue engineering, *Polym. Adv. Technol.* 30 (8) (2019) 2086–2099.
- [58] L. Wang, Y. Wu, T. Hu, B. Guo, P.X. Ma, Electrospun conductive nanofibrous scaffolds for engineering cardiac tissue and 3D bioactuators, *Acta Biomater.* 59 (2017) 68–81.
- [59] H. Wei, X. Cauchy, I.O. Navas, Y. Abderrafai, K. Chizari, U. Sundararaj, Y. Liu, J. Leng, D. Therriault, Direct 3D printing of hybrid nanofiber-based nanocomposites for highly conductive and shape memory applications, *ACS Appl. Mater. Interfaces* 11 (27) (2019) 24523–24532.
- [60] G. Luo, K.S. Teh, Y. Liu, X. Zang, Z. Wen, L. Lin, Direct-write, self-aligned electrospinning on paper for controllable fabrication of three-dimensional structures, *ACS Appl. Mater. Interfaces* 7 (50) (2015) 27765–27770.
- [61] H. Qing, Y. Ji, W. Li, G. Zhao, Q. Yang, X. Zhang, Z. Luo, T.J. Lu, G. Jin, F. Xu, Microfluidic printing of three-dimensional graphene electroactive microfibrous scaffolds, *ACS Appl. Mater. Interfaces* 12 (2) (2020) 2049–2058.
- [62] O.Y. Kweon, S.J. Lee, J.H. Oh, Wearable high-performance pressure sensors based on three-dimensional electrospun conductive nanofibers, *NPG Asia Mater.* 10 (6) (2018) 540–551.
- [63] J.Y. Feng, H. Shi, X.Y. Yang, S. Xiao, Self-adhesion conductive sub-micron fiber cardiac patch from shape memory polymers to promote electrical signal transduction function, *ACS Appl. Mater. Interfaces* 13 (17) (2021) 19593–19602.
- [64] G. Zhao, Y. Feng, L. Xue, M. Cui, Q. Zhang, F. Xu, N. Peng, Z. Jiang, D. Gao, X. Zhang, Anisotropic conductive reduced graphene oxide/silk matrices promote post-infarction myocardial function by restoring electrical integrity, *Acta Biomater.* 139 (2021) 190–203.
- [65] X. Wang, M. Jiang, Z. Zhou, J. Gou, D. Hui, 3D printing of polymer matrix composites: a review and prospective, *Compos. B Eng.* 110 (2017) 442–458.

- [66] J. He, P. Xia, D. Li, Development of melt electrohydrodynamic 3D printing for complex microscale poly (epsilon-caprolactone) scaffolds, *Biofabrication* 8 (3) (2016), 035008.
- [67] K. Chatterjee, T.K. Ghosh, 3D printing of textiles: potential roadmap to printing with fibers, *Adv. Mater.* 32 (4) (2020), 1902086.
- [68] M. Alizadehgiashi, A. Gevorkian, M. Tebbe, M. Seo, E. Prince, E. Kumacheva, 3D-Printed microfluidic devices for materials science, *Adv. Mater. Technol.* 3 (7) (2018), 1800068.
- [69] M.A. Darabi, A. Khosrozadeh, R. Mbeleck, Y. Liu, Q. Chang, J. Jiang, J. Cai, Q. Wang, G. Luo, M. Xing, Skin-inspired multifunctional autonomic-intrinsic conductive self-healing hydrogels with pressure sensitivity, stretchability, and 3D printability, *Adv. Mater.* 29 (31) (2017), 1705922.
- [70] K. Zhu, S.R. Shin, T. van Kempen, Y.C. Li, V. Ponraj, A. Nasajpour, S. Mandla, N. Hu, X. Liu, J. Leijten, Y.D. Lin, M.A. Hussain, Y.S. Zhang, A. Tamayol, A. Khademhosseini, Gold nanocomposite bioink for printing 3D cardiac constructs, *Adv. Funct. Mater.* 27 (12) (2017), 1605352.
- [71] Y. Chen, Z. Deng, R. Ouyang, R. Zheng, Z. Jiang, H. Bai, H. Xue, 3D printed stretchable smart fibers and textiles for self-powered e-skin, *Nano Energy* 84 (2021), 105866.
- [72] Y. Li, H. Zhu, Y. Wang, U. Ray, S. Zhu, J. Dai, C. Chen, K. Fu, S.-H. Jang, D. Henderson, T. Li, L. Hu, Cellulose-nanofiber-enabled 3D printing of a carbon-nanotube microfibrillar network, *Small Methods* 1 (10) (2017), 1700222.
- [73] X.-X. He, J. Zheng, G.-F. Yu, M.-H. You, M. Yu, X. Ning, Y.-Z. Long, Near-field electrospinning: progress and applications, *J. Phys. Chem. C* 121 (16) (2017) 8663–8678.
- [74] D. Sun, C. Chang, S. Li, L. Lin, Near-field electrospinning, *Nano Lett.* 6 (4) (2006) 839–842.
- [75] J. Wang, H.Y. Wang, X.M. Mo, H.J. Wang, Reduced graphene oxide-encapsulated microfibrillar patterns enable controllable formation of neuronal-like networks, *Adv. Mater.* 32 (40) (2020), 2004555.
- [76] I. Liashenko, A. Hrynevich, P.D. Dalton, Designing outside the box: unlocking the geometric freedom of melt electrowriting using microscale layer shifting, *Adv. Mater.* 32 (28) (2020), 2001874.
- [77] J.C. Kade, P.D. Dalton, Polymers for melt electrowriting, *Adv. Mater.* 10 (1) (2021), 2001232.
- [78] J.H.Y. Chung, S. Sayyar, G.G. Wallace, Effect of graphene addition on polycaprolactone scaffolds fabricated using melt-electrowriting, *Polymers* 14 (2) (2022) 319.
- [79] S. Wei, G. Qu, G. Luo, Y. Huang, H. Zhang, X. Zhou, L. Wang, Z. Liu, T. Kong, Scalable and automated fabrication of conductive tough-hydrogel microfibers with ultrastretchability, 3D printability, and stress sensitivity, *ACS Appl. Mater. Interfaces* 10 (13) (2018) 11204–11212.
- [80] P. Parandoush, D. Lin, A review on additive manufacturing of polymer-fiber composites, *Compos. Struct.* 182 (2017) 36–53.
- [81] S.-M. Jeong, J. Yang, J.H. Pak, K. Seo, T. Lim, S. Ju, Real-time information-variable invisible barcode comprising freely deformable infrared-emitting yarns, *ACS Appl. Mater. Interfaces* 13 (34) (2021) 41046–41055.
- [82] Y. Li, Y. Gao, L. Lan, Q. Zhang, L. Wei, M. Shan, L. Guo, F. Wang, J. Mao, Z. Zhang, L. Wang, Ultrastretchable and wearable conductive multifilament enabled by buckled polypyrrole structure in parallel, *NPJ Flexible Electron.* 6 (1) (2022) 42.
- [83] Z. Yang, Z. Zhai, Z. Song, Y. Wu, J. Liang, Y. Shan, J. Zheng, H. Liang, H. Jiang, Conductive and elastic 3D helical fibers for use in washable and wearable electronics, *Adv. Mater.* 32 (10) (2020), 1907495.
- [84] Y. Zhao, Q. Zhai, D. Dong, T. An, S. Gong, Q. Shi, W. Cheng, Highly stretchable and strain-insensitive fiber-based wearable electrochemical biosensor to monitor glucose in the sweat, *Anal. Chem.* 91 (10) (2019) 6569–6576.
- [85] Y. Yang, B. Xu, Y. Gao, M. Li, Conductive composite fiber with customizable functionalities for energy harvesting and electronic textiles, *ACS Appl. Mater. Interfaces* 13 (42) (2021) 49927–49935.
- [86] D. Yang, B. Zhou, G. Han, Y. Feng, J. Ma, J. Han, C. Liu, C. Shen, Flexible transparent polypyrrole-decorated MXene-based film with excellent photothermal energy conversion performance, *ACS Appl. Mater. Interfaces* 13 (7) (2021) 8909–8918.
- [87] X. Zhang, X. Wang, Z. Lei, L. Wang, M. Tian, S. Zhu, H. Xiao, X. Tang, L. Qu, Flexible MXene-decorated fabric with interwoven conductive networks for integrated joule heating, electromagnetic interference shielding, and strain sensing performances, *ACS Appl. Mater. Interfaces* 12 (12) (2020) 14459–14467.
- [88] X. Tang, D. Cheng, J. Ran, D. Li, C. He, S. Bi, G. Cai, X. Wang, Recent advances on the fabrication methods of nanocomposite yarn-based strain sensor, *Nanotechnol. Rev.* 10 (1) (2021) 221–236.
- [89] T. Makowski, M. Svyntkivska, E. Piorkowska, D. Kregiel, Multifunctional polylactide nonwovens with 3D network of multiwall carbon nanotubes, *Appl. Surf. Sci.* 527 (2020), 146898.
- [90] A. Rebelo, Y. Liu, C. Liu, K.H. Schafer, M. Saumer, G. Yang, Poly(4-vinylaniline)/polyaniline bilayer functionalized bacterial cellulose membranes as bioelectronics interfaces, *Carbohydr. Polym.* 204 (2019) 190–201.
- [91] H. Ahmed, T.A. Khattab, H.M. Mashaly, A.A. El-Halwagy, M. Rehan, Plasma activation toward multi-stimuli responsive cotton fabric via in situ development of polyaniline derivatives and silver nanoparticles, *Cellulose* 27 (5) (2020) 2913–2926.
- [92] T. Khatti, H. Naderi-Manesh, S.M. Kalantar, Polypyrrole-coated polycaprolactone-gelatin conductive nanofibers: fabrication and characterization, *Mater. Sci. Eng., B* 250 (2019), 114440.
- [93] Q. Zhang, Y. Qiao, J. Zhu, Y. Li, C. Li, J. Lin, X. Li, H. Han, J. Mao, F. Wang, L. Wang, Electroactive and antibacterial surgical sutures based on chitosan-gelatin/tannic acid/polypyrrole composite coating, *Compos. B Eng.* 223 (2021), 109140.
- [94] W. Jing, Q. Ao, L. Wang, Z. Huang, Q. Cai, G. Chen, X. Yang, W. Zhong, Constructing conductive conduit with conductive fibrous infilling for peripheral nerve regeneration, *Chem. Eng. J.* 345 (2018) 566–577.
- [95] T.H. Park, S. Yu, M. Koo, H. Kim, E.H. Kim, J.-E. Park, B. Ok, B. Kim, S.H. Noh, C. Park, E. Kim, C.M. Koo, C. Park, Shape-adaptable 2D titanium carbide (MXene) heater, *ACS Nano* 13 (6) (2019) 6835–6844.
- [96] B. Wang, S. Bao, S. Vinnikova, P. Ghanta, S. Wang, Buckling analysis in stretchable electronics, *NPJ Flexible Electron.* 1 (1) (2017) 5.
- [97] F. Sun, M. Tian, X. Sun, T. Xu, X. Liu, S. Zhu, X. Zhang, L. Qu, Stretchable conductive fibers of ultrahigh tensile strain and stable conductance enabled by a worm-shaped graphene microlayer, *Nano Lett.* 19 (9) (2019) 6592–6599.
- [98] Z.F. Liu, S. Fang, F.A. Moura, J.N. Ding, N. Jiang, J. Di, M. Zhang, X. Lepró, D. S. Galvão, C.S. Haines, N.Y. Yuan, S.G. Yin, D.W. Lee, R. Wang, H.Y. Wang, W. Lv, C. Dong, R.C. Zhang, M.J. Chen, Q. Yin, Y.T. Chong, R. Zhang, X. Wang, M. D. Lima, R. Ovalle-Robles, D. Qian, H. Lu, R.H. Baughman, Hierarchically buckled sheath-core fibers for superelastic electronics, sensors, and muscles, *Science* 349 (6246) (2015) 400–404.
- [99] Q. Li, C. Ding, W. Yuan, R. Xie, X. Zhou, Y. Zhao, M. Yu, Z. Yang, J. Sun, Q. Tian, F. Han, H. Li, X. Deng, G. Li, Z. Liu, Highly stretchable and permeable conductors based on shrinkable electrospun fiber mats, *Adv. Fiber Mater.* 3 (5) (2021) 302–311.
- [100] Y. Li, Y. Xiao, C. Liu, The horizon of materiobiology: a perspective on material-guided cell behaviors and tissue engineering, *Chem. Rev.* 117 (5) (2017) 4376–4421.
- [101] S. Seyedin, S. Uzun, A. Levitt, B. Anasori, G. Dion, Y. Gogotsi, J.M. Razal, MXene composite and coaxial fibers with high stretchability and conductivity for wearable strain sensing textiles, *Adv. Funct. Mater.* 30 (12) (2020), 1910504.
- [102] G. Zhao, H. Qing, G. Huang, G.M. Genin, T.J. Lu, Z. Luo, F. Xu, X. Zhang, Reduced graphene oxide functionalized nanofibrous silk fibroin matrices for engineering excitable tissues, *NPG Asia Mater.* 10 (10) (2018) 982–994.
- [103] Y.B. Wu, L. Wang, B.L. Guo, P.X. Ma, Interwoven aligned conductive nanofiber yarn/hydrogel composite scaffolds for engineered 3D cardiac anisotropy, *ACS Nano* 11 (6) (2017) 5646–5659.
- [104] R.D. Pedde, B. Mirani, A. Navaei, T. Styran, S. Wong, M. Mehrali, A. Thakur, N. K. Mohtaram, A. Bayati, A. Dolatshahi-Pirouz, M. Nikkha, S.M. Willerth, M. Akbari, Emerging biofabrication strategies for engineering complex tissue constructs, *Adv. Mater.* 29 (19) (2017), 1606061.
- [105] B. Ozkale, M.S. Sakar, D.J. Mooney, Active biomaterials for mechanobiology, *Biomaterials* 267 (2021), 120497.
- [106] J. Zonderland, L. Moroni, Steering cell behavior through mechanobiology in 3D: a regenerative medicine perspective, *Biomaterials* 268 (2021), 120572.
- [107] M. Tewary, P.W. Zandstra, Mechanics-guided developmental fate patterning, *Nat. Mater.* 17 (7) (2018) 571–572.
- [108] Y. Kong, J. Duan, F. Liu, L. Han, G. Li, C. Sun, Y. Sang, S. Wang, F. Yi, H. Liu, Regulation of stem cell fate using nanostructure-mediated physical signals, *Chem. Soc. Rev.* 50 (22) (2021) 12828–12872.
- [109] D.M. dos Santos, D.S. Correa, E.S. Medeiros, J.E. Oliveira, L.H.C. Mattoso, Advances in functional polymer nanofibers: from spinning fabrication techniques to recent biomedical applications, *ACS Appl. Mater. Interfaces* 12 (41) (2020) 45673–45701.
- [110] G.C. Engelmayr, M.Y. Cheng, C.J. Bettinger, J.T. Borenstein, R. Langer, L.E. Freed, Accordion-like honeycombs for tissue engineering of cardiac anisotropy, *Nat. Mater.* 7 (12) (2008) 1003–1010.
- [111] P.P. Lunkenheimer, K. Redmann, N. Kling, X.J. Jiang, K. Rothaus, C.W. Cryer, F. Wubbeling, P. Niederer, P.U. Heitz, S.Y. Ho, R.H. Anderson, Three-dimensional architecture of the left ventricular myocardium, *Anat. Rec. Part A-Discoveries in Molecular Cellular and Evolutionary Biology* 288A (6) (2006) 565–578.
- [112] M. Kharazija, S.R. Shin, M. Nikkha, S.N. Topkaya, N. Masoumi, M. Annabi, M. R. Dokmeci, A. Khademhosseini, Tough and flexible CNT-polymeric hybrid scaffolds for engineering cardiac constructs, *Biomaterials* 35 (26) (2014) 7346–7354.
- [113] Y.W. Liu, J.F. Lu, G.S. Xu, J.J. Wei, Z.B. Zhang, X.H. Li, Tuning the conductivity and inner structure of electrospun fibers to promote cardiomyocyte elongation and synchronous beating, *Mater. Sci. Eng. C* 69 (2016) 865–874.
- [114] C. Zhang, M.-H. Hsieh, S.-Y. Wu, S.-H. Li, J. Wu, S.-M. Liu, H.-J. Wei, R.D. Weisel, H.-W. Sung, R.-K. Li, A self-doping conductive polymer hydrogel that can restore electrical impulse propagation at myocardial infarct to prevent cardiac arrhythmia and preserve ventricular function, *Biomaterials* 231 (2020), 119672.
- [115] T. Wu, C. Cui, Y. Huang, Y. Liu, C. Fan, X. Han, Y. Yang, Z. Xu, B. Liu, G. Fan, W. Liu, Coadministration of an adhesive conductive hydrogel patch and an injectable hydrogel to treat myocardial infarction, *ACS Appl. Mater. Interfaces* 12 (2) (2020) 2039–2048.
- [116] M.H. Norahan, M. Pourmokhtari, M.R. Saeb, B. Bakhshi, M. Soufi Zomorrod, N. Baheiraei, Electroactive cardiac patch containing reduced graphene oxide with potential antibacterial properties, *Mater. Sci. Eng. C* 104 (2019), 109921.
- [117] G. Zhao, X. Zhang, B. Li, G. Huang, F. Xu, X. Zhang, Solvent-free fabrication of carbon nanotube/silk fibroin electrospun matrices for enhancing cardiomyocyte functionalities, *ACS Biomater. Sci. Eng.* 6 (3) (2020) 1630–1640.
- [118] K. Roshanbifar, L. Vogt, F. Ruther, J.A. Roether, A.R. Boccacini, F.B. Engel, Nanofibrous composite with tailorable electrical and mechanical properties for cardiac tissue engineering, *Adv. Funct. Mater.* 30 (7) (2020), 1908612.
- [119] A.K. Capulli, L.A. MacQueen, S.P. Sheehy, K.K. Parker, Fibrous scaffolds for building hearts and heart parts, *Adv. Drug Deliv. Rev.* 96 (2016) 83–102.

- [120] J.X. Ding, J. Zhang, J.N. Li, D. Li, C.S. Xiao, H.H. Xiao, H.H. Yang, X.L. Zhuang, X. S. Chen, Electrospun polymer biomaterials, *Prog. Polym. Sci.* 90 (2019) 1–34.
- [121] M. Castilho, A. van Mil, M. Maher, C.H.G. Metz, G. Hochleitner, J. Groll, P. A. Doevdans, K. Ito, J.P.G. Sluijter, J. Malda, Melt electrowriting allows tailored microstructural and mechanical design of scaffolds to advance functional human myocardial tissue formation, *Adv. Funct. Mater.* 28 (40) (2018), 1803151.
- [122] C.H. Wu, A. Liu, S.P. Chen, X.F. Zhang, L. Chen, Y.D. Zhu, Z.W. Xiao, J. Sun, H. R. Luo, H.S. Fan, Cell-laden electroconductive hydrogel simulating nerve matrix to deliver electrical cues and promote neurogenesis, *ACS Appl. Mater. Interfaces* 11 (25) (2019) 22152–22163.
- [123] C. Meng, W. Jiang, Z. Huang, T. Liu, J. Feng, Fabrication of a highly conductive silk knitted composite scaffold by two-step electrostatic self-assembly for potential peripheral nerve regeneration, *ACS Appl. Mater. Interfaces* 12 (10) (2020) 12317–12327.
- [124] J. Zhang, X. Zhang, C. Wang, F. Li, Z. Qiao, L. Zeng, Z. Wang, H. Liu, J. Ding, H. Yang, Conductive composite fiber with optimized alignment guides neural regeneration under electrical stimulation, *Adv. Healthc. Mater.* 10 (3) (2021), 2000604.
- [125] S. Houshyar, A. Bhattacharyya, R. Shanks, Peripheral nerve conduit: materials and structures, *ACS Chem. Neurosci.* 10 (8) (2019) 3349–3365.
- [126] C. Huang, Y.M. Ouyang, H.T. Niu, N.F. He, Q.F. Ke, X.Y. Jin, D.W. Li, J. Fang, W. J. Liu, C.Y. Fan, T. Lin, Nerve guidance conduits from aligned nanofibers: improvement of nerve regeneration through longitudinal nanogrooves on a fiber surface, *ACS Appl. Mater. Interfaces* 7 (13) (2015) 7189–7196.
- [127] W. Daly, L. Yao, D. Zeugolis, A. Windebank, A. Pandit, A biomaterials approach to peripheral nerve regeneration: bridging the peripheral nerve gap and enhancing functional recovery, *J. R. Soc. Interface* 9 (67) (2012) 202–221.
- [128] P. Sensharma, G. Madhumathi, R.D. Jayant, A.K. Jaiswal, Biomaterials and cells for neural tissue engineering: current choices, *Mater. Sci. Eng. C* 77 (2017) 1302–1315.
- [129] A.C. Pinho, A.C. Fonseca, A.C. Serra, J.D. Santos, J.F.J. Coelho, Peripheral nerve regeneration: current status and new strategies using polymeric materials, *Adv. Healthc. Mater.* 5 (21) (2016) 2732–2744.
- [130] L. Zhu, S.J. Jia, T.J. Liu, L. Yan, D.G. Huang, Z.Y. Wang, S. Chen, Z.P. Zhang, W. Zeng, Y. Zhang, H. Yang, D.J. Hao, Aligned PCL fiber conduits immobilized with nerve growth factor gradients enhance and direct sciatic nerve regeneration, *Adv. Funct. Mater.* 30 (39) (2020), 2002610.
- [131] Y. Zhang, X. Liu, L. Zeng, J. Zhang, J. Zuo, J. Zou, J. Ding, X. Chen, Polymer fiber scaffolds for bone and cartilage tissue engineering, *Adv. Funct. Mater.* 29 (36) (2019), 1903279.
- [132] D. Kim, S.A. Han, J.H. Kim, J.-H. Lee, S.-W. Kim, S.-W. Lee, Biomolecular piezoelectric materials: from amino acids to living tissues, *Adv. Mater.* 32 (14) (2020), 1906989.
- [133] A.H. Rajabi, M. Jaffe, T.L. Arinzech, Piezoelectric materials for tissue regeneration: a review, *Acta Biomater.* 24 (2015) 12–23.
- [134] A.G. Gueux, J.L. Puetzer, A. Armgarth, E. Littmann, E. Stavrinidou, E.P. Giannelis, G.G. Malliaras, M.M. Stevens, Highly porous scaffolds of PEDOT:PSS for bone tissue engineering, *Acta Biomater.* 62 (2017) 91–101.
- [135] Y. Yang, X. Ding, T. Zou, G. Peng, H. Liu, Y. Fan, Preparation and characterization of electrospun graphene/silk fibroin conductive fibrous scaffolds, *RSC Adv.* 7 (13) (2017) 7954–7963.
- [136] H. Nekounam, Z. Allahyari, S. Gholizadeh, E. Mirzaei, M.A. Shokrgozar, R. Faridi-Majidi, Simple and robust fabrication and characterization of conductive carbonized nanofibers loaded with gold nanoparticles for bone tissue engineering applications, *Mater. Sci. Eng. C* 117 (2020), 111226.
- [137] D.K. Patel, Y.-R. Seo, S.D. Dutta, K.-T. Lim, Enhanced osteogenesis of mesenchymal stem cells on electrospun cellulose nanocrystals/poly(ϵ -caprolactone) nanofibers on graphene oxide substrates, *RSC Adv.* 9 (62) (2019) 36040–36049.
- [138] J. Chen, M. Yu, B. Guo, P.X. Ma, Z. Yin, Conductive nanofibrous composite scaffolds based on in-situ formed polyaniline nanoparticle and polylactide for bone regeneration, *J. Colloid Interface Sci.* 514 (2018) 517–527.
- [139] X. Liu, M.N. George, S. Park, A.L. Miller II, B. Gaijre, L. Li, B.E. Waletzki, A. Terzic, M.J. Yaszemski, L. Lu, 3D-printed scaffolds with carbon nanotubes for bone tissue engineering: fast and homogeneous one-step functionalization, *Acta Biomater.* 111 (2020) 129–140.
- [140] B. Huang, C. Vyas, J.J. Byun, M. El-Newehy, Z. Huang, P. Bártolo, Aligned multi-walled carbon nanotubes with nanohydroxyapatite in a 3D printed polycaprolactone scaffold stimulates osteogenic differentiation, *Mater. Sci. Eng. C* 108 (2020), 110374.
- [141] B. Maharjan, V.K. Kaliannagounder, S.R. Jang, G.P. Awasthi, D.P. Bhattarai, G. Choukrani, C.H. Park, C.S. Kim, In-situ polymerized polypyrrole nanoparticles immobilized poly(ϵ -caprolactone) electrospun conductive scaffolds for bone tissue engineering, *Mater. Sci. Eng. C* 114 (2020), 111056.
- [142] E.P. E Silva, B. Huang, J.V. Helaeihl, P.R.L. Nalesso, L. Bagne, M.A. De Oliveira, G.C.C. Albiazetti, A. Aldabahi, M. El-Newehy, M. Santamaria Jr., F.A. S. Mendonça, P. Bártolo, G.F. Caetano, In vivo study of conductive 3D printed PCL/MWCNTs scaffolds with electrical stimulation for bone tissue engineering, *Bio-Design. Manuf.* 4 (2) (2021) 190–202.
- [143] Z. Jia, J. Gong, Y. Zeng, J. Ran, J. Liu, K. Wang, C. Xie, X. Lu, J. Wang, Bioinspired conductive silk microfiber integrated bioelectronic for diagnosis and wound healing in diabetes, *Adv. Funct. Mater.* 31 (19) (2021), 2010461.
- [144] A. Memic, T. Abudula, H.S. Mohammed, K. Joshi Navare, T. Colombani, S. A. Bencherif, Latest progress in electrospun nanofibers for wound healing applications, *ACS Appl. Bio Mater.* 2 (3) (2019) 952–969.
- [145] S. Homaeigohar, A.R. Boccaccini, Antibacterial biohybrid nanofibers for wound dressings, *Acta Biomater.* 107 (2020) 25–49.
- [146] J.-X. Liu, W.-H. Dong, X.-J. Mou, G.-S. Liu, X.-W. Huang, X. Yan, C.-F. Zhou, S. Jiang, Y.-Z. Long, In situ electrospun zein/thyme essential oil-based membranes as an effective antibacterial wound dressing, *ACS Appl. Bio Mater.* 3 (1) (2020) 302–307.
- [147] R. Singh, S. Khan, S.M. Basu, M. Chauhan, N. Sarviya, J. Giri, Fabrication, characterization, and biological evaluation of airbrushed gelatin nanofibers, *ACS Appl. Bio Mater.* 2 (12) (2019) 5340–5348.
- [148] Y. Xi, J. Ge, M. Wang, M. Chen, W. Niu, W. Cheng, Y. Xue, C. Lin, B. Lei, Bioactive anti-inflammatory, antibacterial, antioxidative silicon-based nanofibrous dressing enables cutaneous tumor photothermo-chemo therapy and infection-induced wound healing, *ACS Nano* 14 (3) (2020) 2904–2916.
- [149] J. He, Y. Liang, M. Shi, B. Guo, Anti-oxidant electroactive and antibacterial nanofibrous wound dressings based on poly(ϵ -caprolactone)/quaternized chitosan-graft-polyaniline for full-thickness skin wound healing, *Chem. Eng. J.* 385 (2020), 123464.
- [150] T.H. Qazi, R. Rai, A.R. Boccaccini, Tissue engineering of electrically responsive tissues using polyaniline based polymers: a review, *Biomaterials* 35 (33) (2014) 9068–9086.
- [151] X.J. Chen, D.D. Hou, L. Wang, Q. Zhang, J.H. Zou, G. Sun, Antibacterial surgical silk sutures using a high-performance slow-release carrier coating system, *ACS Appl. Mater. Interfaces* 7 (40) (2015) 22394–22403.
- [152] Y. Lee, H. Kim, Y. Kim, S. Noh, B. Chun, J. Kim, C. Park, M. Choi, K. Park, J. Lee, J. Seo, A multifunctional electronic suture for continuous strain monitoring and on-demand drug release, *Nanoscale* 13 (43) (2021) 18112–18124.
- [153] V. Kalidasan, X. Yang, Z. Xiong, R.R. Li, H.C. Yao, H. Godaba, S. Obuobi, P. Singh, X. Guan, X. Tian, S.A. Kurt, Z.P. Li, D. Mukherjee, R. Rajarethinam, C.S. Chong, J. W. Wang, P.L.R. Ee, W.Q. Loke, B.C.K. Tee, J.Y. Ouyang, C.J. Charles, J.S. Ho, Wirelessly operated bioelectronic sutures for the monitoring of deep surgical wounds, *Nat. Biomed. Eng.* 5 (10) (2021) 1217–1227.
- [154] T. Someya, Z. Bao, G.G. Malliaras, The rise of plastic bioelectronics, *Nature* 540 (7633) (2016) 379–385.
- [155] X. Wu, J. Feng, J. Deng, Z. Cui, L. Wang, S. Xie, C. Chen, C. Tang, Z. Han, H. Yu, X. Sun, H. Peng, Fiber-shaped organic electrochemical transistors for biochemical detections with high sensitivity and stability, *Sci. China Chem.* 63 (9) (2020) 1281–1288.
- [156] A. Canales, S. Park, A. Kilias, P. Anikeeva, Multifunctional fibers as tools for neuroscience and neuroengineering, *Accounts Chem. Res.* 51 (4) (2018) 829–838.
- [157] C. Tang, S. Xie, M. Wang, J. Peng, Z. Han, X. Wu, L. Wang, C. Chen, J. Wang, L. Jiang, P. Chen, X. Sun, H. Peng, A fiber-shaped neural probe with alterable elastic moduli for direct implantation and stable electronic-brain interfaces, *J. Mater. Chem. B* 8 (20) (2020) 4387–4394.
- [158] J. Yu, W. Ling, Y. Li, N. Ma, Z. Wu, R. Liang, H. Pan, W. Liu, B. Fu, K. Wang, C. Li, H. Wang, H. Peng, B. Ning, J. Yang, X. Huang, A multichannel flexible optoelectronic fiber device for distributed implantable neurological stimulation and monitoring, *Small* 17 (4) (2021), e2005925.
- [159] A. Ahmed, M.M. Hossain, B. Adak, S. Mukhopadhyay, Recent advances in 2D MXene integrated smart-textile interfaces for multifunctional applications, *Chem. Mater.* 32 (24) (2020) 10296–10320.
- [160] J.S. Choi, H.J. Lee, S. Rajaraman, D.H. Kim, Recent advances in three-dimensional microelectrode array technologies for in vitro and in vivo cardiac and neuronal interfaces, *Biosens. Bioelectron.* 171 (2021), 112687.
- [161] X. Zheng, K.M. Woeppel, A.Y. Griffith, E. Chang, M.J. Looker, L.E. Fisher, B. J. Clapsaddle, X.T. Cui, Soft conducting elastomer for peripheral nerve interface, *Adv. Healthc. Mater.* 8 (9) (2019), 1801311.
- [162] C. Lu, S. Park, T.J. Richner, A. Derry, I. Brown, C. Hou, S. Rao, J. Kang, C. T. Moritz, Y. Fink, P. Anikeeva, Flexible and stretchable nanowire-coated fibers for optoelectronic probing of spinal cord circuits, *Sci. Adv.* 3 (2017), e1600955.
- [163] S. Jiang, J. Song, Y. Zhang, M. Nie, J. Kim, A.L. Marciano, K. Kadlec, W.A. Mills III, X. Yan, H. Liu, R. Tong, H. Wang, I.F. Kimbrough, H. Sontheimer, W. Zhou, X. Jia, Nano-optoelectrodes integrated with flexible multifunctional fiber probes by high-throughput scalable fabrication, *ACS Appl. Mater. Interfaces* 13 (7) (2021) 9156–9165.
- [164] T.J. Mun, S.H. Kim, J.W. Park, J.H. Moon, Y. Jang, C. Huynh, R.H. Baughman, S. J. Kim, Wearable energy generating and storing textile based on carbon nanotube yarns, *Adv. Funct. Mater.* 30 (23) (2020), 2000411.
- [165] J.Y. Lee, D.-g. Cho, S.-P. Cho, J.-H. Choi, S.-J. Sung, S. Hong, W.-R. Yu, Semiconducting carbon nanotube fibers for electrochemical biosensor platforms, *Mater. Des.* 192 (2020), 108740.
- [166] Y.C. Zhou, X.M. Lin, Z. Yang, X.T. Han, M. Liu, Fabrication of a lead head made of the carbon-fiber-reinforced composite for the temporary cardiac pacemaker, *2021, Bioinorgan. Chem. Appl.* (2021), 7507555.
- [167] C. Hang, L. Ding, S. Cheng, R. Dong, J. Qi, X. Liu, Q. Liu, Y. Zhang, X. Jiang, A soft and absorbable temporary epicardial pacing wire, *Acta Biomater.* 33 (36) (2021), 2101447.
- [168] H. Sheng, X. Zhang, J. Liang, M. Shao, E. Xie, C. Yu, W. Lan, Recent advances of energy solutions for implantable bioelectronics, *Adv. Healthc. Mater.* 10 (17) (2021), 2100199.
- [169] D. Yu, Q. Qian, L. Wei, W. Jiang, K. Goh, J. Wei, J. Zhang, Y. Chen, Emergence of fiber supercapacitors, *Chem. Soc. Rev.* 44 (3) (2015) 647–662.
- [170] Y. Hu, H. Cheng, F. Zhao, N. Chen, L. Jiang, Z. Feng, L. Qu, All-in-one graphene fiber supercapacitor, *Nanoscale* 6 (12) (2014) 6448.
- [171] H.J. Sim, C. Choi, D.Y. Lee, H. Kim, J.-H. Yun, J.M. Kim, T.M. Kang, R. Ovalle, R. H. Baughman, C.W. Kee, S.J. Kim, Biomolecule based fiber supercapacitor for implantable device, *Nano Energy* 47 (2018) 385–392.

- [172] S. He, Y. Hu, J. Wan, Q. Gao, Y. Wang, S. Xie, L. Qiu, C. Wang, G. Zheng, B. Wang, H. Peng, Biocompatible carbon nanotube fibers for implantable supercapacitors, *Carbon* 122 (2017) 162–167.
- [173] Y. Jang, T. Park, E. Kim, J.W. Park, D.Y. Lee, S.J. Kim, Implantable biosupercapacitor inspired by the cellular redox system, *Angew. Chem., Int. Ed.* 60 (19) (2021) 10563–10567.
- [174] Q.Q. Niu, X.Y. Huang, S.S. Lv, X. Yao, S.N. Fan, Y.P. Zhang, Natural polymer-based bioabsorbable conducting wires for implantable bioelectronic devices, *J. Mater. Chem.* 8 (47) (2020) 25323–25335.
- [175] W.H. Zuo, R.Z. Li, C. Zhou, Y.Y. Li, J.L. Xia, J.P. Liu, Battery-supercapacitor hybrid devices: recent progress and future prospects, *Adv. Sci.* 4 (7) (2017), 1600539.
- [176] J. Sun, Y. Huang, C. Fu, Z. Wang, Y. Huang, M. Zhu, C. Zhi, H. Hu, High-performance stretchable yarn supercapacitor based on PPy@CNTs@urethane elastic fiber core spun yarn, *Nano Energy* 27 (2016) 230–237.
- [177] H. Shi, S. Chen, W. Shi, Z. Peng, J. Li, Z. Liu, G. Zhang, L. Liu, High performance fiber-shaped supercapacitors based on core-shell fiber electrodes with adjustable surface wrinkles and robust interfaces, *J. Mater. Chem.* 9 (31) (2021) 16852–16859.
- [178] Q. Zhang, J. Sun, Z. Pan, J. Zhang, J. Zhao, X. Wang, C. Zhang, Y. Yao, W. Lu, Q. Li, Y. Zhang, Z. Zhang, Stretchable fiber-shaped asymmetric supercapacitors with ultrahigh energy density, *Nano Energy* 39 (2017) 219–228.
- [179] X. Zheng, X. Zhou, J. Xu, L. Zou, W. Nie, X. Hu, S. Dai, Y. Qiu, N. Yuan, Highly stretchable CNT/MnO₂ nanosheets fiber supercapacitors with high energy density, *J. Mater. Sci.* 55 (19) (2020) 8251–8263.
- [180] H. Xie, G. Luo, Y. Niu, W. Weng, Y. Zhao, Z. Ling, C. Ruan, G. Li, W. Sun, Synthesis and utilization of Co₃O₄ doped carbon nanofiber for fabrication of hemoglobin-based electrochemical sensor, *Mater. Sci. Eng. C* 107 (2020), 110209.
- [181] L.A. Mercante, A. Pavinatto, L.E.O. Iwaki, V.P. Scagion, V. Zucolotto, O. N. Oliveira, L.H.C. Mattoso, D.S. Correa, Electrospun polyamide 6/Poly (allylamine hydrochloride) nanofibers functionalized with carbon nanotubes for electrochemical detection of dopamine, *ACS Appl. Mater. Interfaces* 7 (8) (2015) 4784–4790.
- [182] L.Y. Wang, S.L. Xie, Z.Y. Wang, F. Liu, Y.F. Yang, C.Q. Tang, X.Y. Wu, P. Liu, Y. J. Li, H. Saiyin, S. Zheng, X.M. Sun, F. Xu, H.B. Yu, H.S. Peng, Functionalized helical fibre bundles of carbon nanotubes as electrochemical sensors for long-term in vivo monitoring of multiple disease biomarkers, *Nat. Biomed. Eng.* 4 (2) (2020) 159–171.
- [183] T.E. Kerr-Phillips, N. Aydemir, E.W.C. Chan, D. Barker, J. Malmstrom, C. Plesse, J. Travas-Sejdic, Conducting electrospun fibres with polyanionic grafts as highly selective, label-free, electrochemical biosensor with a low detection limit for non-Hodgkin lymphoma gene, *Biosens. Bioelectron.* 100 (2018) 549–555.
- [184] C.G. Sanz, M. Onea, A. Aldea, M.M. Barsan, Disposable superoxide dismutase biosensors based on gold covered polycaprolactone fibers for the detection of superoxide in cell culture media, *Talanta* 241 (2022), 123255.
- [185] Y. Jiang, M. Xu, V.K. Yadavalli, Silk fibroin-sheathed conducting polymer wires as organic connectors for biosensors, *Biosensors* 9 (3) (2019) 103.
- [186] G. Chen, H. Wang, R. Guo, M. Duan, Y. Zhang, J. Liu, Superelastic EGaIn composite fibers sustaining 500% tensile strain with superior electrical conductivity for wearable electronics, *ACS Appl. Mater. Interfaces* 12 (5) (2020) 6112–6118.
- [187] L. Zheng, M. Zhu, B. Wu, Z. Li, S. Sun, P. Wu, Conductance-stable liquid metal sheath-core microfibers for stretchy smart fabrics and self-powered sensing, *Sci. Adv.* 7 (22) (2021), eabg4041.
- [188] T. Kim, C. Park, E.P. Samuel, S. An, A. Aldabahi, F. Alotaibi, A.L. Yarin, S. Yoon, Supersonically sprayed washable, wearable, stretchable, hydrophobic, and antibacterial rGO/AgNW fabric for multifunctional sensors and supercapacitors, *ACS Appl. Mater. Interfaces* 13 (8) (2021) 10013–10025.
- [189] X. Zhao, L.Y. Wang, C.Y. Tang, X.J. Zha, Y. Liu, B.H. Su, K. Ke, R.Y. Bao, M. B. Yang, W. Yang, Smart Ti3C₂Tx MXene fabric with fast humidity response and joule heating for healthcare and medical therapy applications, *ACS Nano* 14 (7) (2020) 8793–8805.
- [190] J. Li, L. Wang, X. Wang, Y. Yang, Z. Hu, L. Liu, Y. Huang, Highly conductive PVA/Ag coating by aqueous in situ reduction and its stretchable structure for strain sensor, *ACS Appl. Mater. Interfaces* 12 (1) (2020) 1427–1435.
- [191] R. Wu, L. Ma, C. Hou, Z. Meng, W. Guo, W. Yu, R. Yu, F. Hu, X.Y. Liu, Silk composite electronic textile sensor for high space precision 2D combo temperature–pressure sensing, *Small* 15 (31) (2019), 1901558.
- [192] G. Yun, S.-Y. Tang, Q. Zhao, Y. Zhang, H. Lu, D. Yuan, S. Sun, L. Deng, M. D. Dickey, W. Li, Liquid metal composites with anisotropic and unconventional piezoconductivity, *Matter* 3 (3) (2020) 824–841.
- [193] F.G.J. Oosterveld, J.J. Rasker, Effects of local heat and cold treatment on surface and articular temperature of arthritic knees, *Arthritis Rheum.* 37 (11) (1994) 1576–1582.
- [194] Y.Q. Li, W.B. Zhu, X.G. Yu, P. Huang, S.Y. Fu, N. Hu, K. Liao, Multifunctional wearable device based on flexible and conductive carbon sponge/polydimethylsiloxane composite, *ACS Appl. Mater. Interfaces* 8 (48) (2016) 33189–33196.
- [195] Y. Li, Z. Zhang, X. Li, J. Zhang, H. Lou, X. Shi, X. Cheng, H. Peng, A smart, stretchable resistive heater textile, *J. Mater. Chem. C* 5 (1) (2017) 41–46.
- [196] M. Zhang, C. Wang, X. Liang, Z. Yin, K. Xia, H. Wang, M. Jian, Y. Zhang, Weft-knitted fabric for a highly stretchable and low-voltage wearable heater, *Adv. Electron. Mater.* 3 (9) (2017), 1700193.
- [197] X. Wang, Z. Lei, X. Ma, G. He, T. Xu, J. Tan, L. Wang, X. Zhang, L. Qu, X. Zhang, A lightweight MXene-Coated nonwoven fabric with excellent flame Retardancy, EMI Shielding, and Electrothermal/Photothermal conversion for wearable heater, *Chem. Eng. J.* 430 (2022), 132605.
- [198] J. Dong, S. Luo, S. Ning, G. Yang, D. Pan, Y. Ji, Y. Feng, F. Su, C. Liu, MXene-coated wrinkled fabrics for stretchable and multifunctional electromagnetic interference shielding and electro/photo-thermal conversion applications, *ACS Appl. Mater. Interfaces* 13 (50) (2021) 60478–60488.
- [199] Y. Cheng, H. Zhang, R. Wang, X. Wang, H. Zhai, T. Wang, Q. Jin, J. Sun, Highly stretchable and conductive copper nanowire based fibers with hierarchical structure for wearable heaters, *ACS Appl. Mater. Interfaces* 8 (48) (2016) 32925–32933.
- [200] Q. Liu, B. Tian, J. Liang, W. Wu, Recent advances in printed flexible heaters for portable and wearable thermal management, *Mater. Horiz.* 8 (6) (2021) 1634–1656.
- [201] C. Ye, J. Ren, Y. Wang, W. Zhang, C. Qian, J. Han, C. Zhang, K. Jin, M.J. Buehler, D.L. Kaplan, S. Ling, Design and fabrication of silk templated electronic yarns and applications in multifunctional textiles, *Matter* 1 (5) (2019) 1411–1425.
- [202] K. Kang, J. Park, K. Kim, K.J. Yu, Recent developments of emerging inorganic, metal and carbon-based nanomaterials for pressure sensors and their healthcare monitoring applications, *Nano Res.* 14 (9) (2021) 3096–3111.
- [203] L. Chen, M. Lu, H. Yang, J.R. Salas Avila, B. Shi, L. Ren, G. Wei, X. Liu, W. Yin, Textile-based capacitive sensor for physical rehabilitation via surface topological modification, *ACS Nano* 14 (7) (2020) 8191–8201.
- [204] L. Li, H. Xiang, Y. Xiong, H. Zhao, Y. Bai, S. Wang, F. Sun, M. Hao, L. Liu, T. Li, Z. Peng, J. Xu, T. Zhang, Ultrastretchable fiber sensor with high sensitivity in whole workable range for wearable electronics and implantable medicine, *Adv. Sci.* 5 (9) (2018), 1800558.
- [205] Z. Li, X. Qi, L. Xu, H. Lu, W. Wang, X. Jin, Z.I. Md, Y. Zhu, Y. Fu, Q. Ni, Y. Dong, Self-repairing, large linear working range shape memory carbon nanotubes/ethylene vinyl acetate fiber strain sensor for human movement monitoring, *ACS Appl. Mater. Interfaces* 12 (37) (2020) 42179–42192.
- [206] J.-H. Pu, X. Zhao, X.-J. Zha, L. Bai, K. Ke, R.-Y. Bao, Z.-Y. Liu, M.-B. Yang, W. Yang, Multilayer structured AgNW/WPU-MXene fiber strain sensors with ultrahigh sensitivity and a wide operating range for wearable monitoring and healthcare, *J. Mater. Chem.* 7 (26) (2019) 15913–15923.
- [207] M. Gong, L. Yue, J. Kong, X. Lin, L. Zhang, J. Wang, D. Wang, Knittable and sewable spandex yarn with nacre-mimetic composite coating for wearable health monitoring and thermo- and antibacterial therapies, *ACS Appl. Mater. Interfaces* 13 (7) (2021) 9053–9063.
- [208] J. Chen, J. Zhang, J. Hu, N. Luo, F. Sun, H. Venkatesan, N. Zhao, Y. Zhang, Ultrafast-response/recovery flexible piezoresistive sensors with DNA-like double helix yarns for epidermal pulse monitoring, *Adv. Mater.* 34 (2) (2021), 2104313.
- [209] S. Yang, C. Li, N. Wen, S. Xu, H. Huang, T. Cong, Y. Zhao, Z. Fan, K. Liu, L. Pan, All-fabric-based multifunctional textile sensor for detection and discrimination of humidity, temperature, and strain stimuli, *J. Mater. Chem. C* 9 (39) (2021) 13789–13798.
- [210] Z. Hui, R. Chen, J. Chang, Y. Gong, X. Zhang, H. Xu, Y. Sun, Y. Zhao, L. Wang, R. Zhou, F. Ju, Q. Chen, J. Zhou, J. An, G. Sun, W. Huang, Solution-processed sensing textiles with adjustable sensitivity and linear detection range enabled by twisting structure, *ACS Appl. Mater. Interfaces* 12 (10) (2020) 12155–12164.
- [211] H. Souri, D. Bhattacharyya, Highly stretchable multifunctional wearable devices based on conductive cotton and wool fabrics, *ACS Appl. Mater. Interfaces* 10 (24) (2018) 20845–20853.
- [212] X. Zheng, Q. Hu, Z. Wang, W. Nie, P. Wang, C. Li, Roll-to-roll layer-by-layer assembly bark-shaped carbon nanotube/Ti3C₂Tx MXene textiles for wearable electronics, *J. Colloid Interface Sci.* 602 (2021) 680–688.
- [213] Y. Zheng, R. Yin, Y. Zhao, H. Liu, D. Zhang, X. Shi, B. Zhang, C. Liu, C. Shen, Conductive MXene/cotton fabric based pressure sensor with both high sensitivity and wide sensing range for human motion detection and E-skin, *Chem. Eng. J.* 420 (2021), 127720.
- [214] T. Li, L. Chen, X. Yang, X. Chen, Z. Zhang, T. Zhao, X. Li, J. Zhang, A flexible pressure sensor based on an MXene–textile network structure, *J. Mater. Chem. C* 7 (4) (2019) 1022–1027.
- [215] W. Geng, T.J. Cuthbert, C. Menon, Conductive thermoplastic elastomer composite capacitive strain sensors and their application in a wearable device for quantitative joint angle prediction, *ACS. Appl. Polym. Mater.* 3 (1) (2020) 122–129.
- [216] J. Lee, S.J. Ihle, G.S. Pellegrino, H. Kim, J. Yea, C.-Y. Jeon, H.-C. Son, C. Jin, D. Eberli, F. Schmid, B.L. Zambano, A.F. Renz, C. Forró, H. Choi, K.-I. Jang, R. Küng, J. Vörös, Stretchable and suturable fibre sensors for wireless monitoring of connective tissue strain, *Nat. Electron.* 4 (4) (2021) 291–301.
- [217] S. Uzun, S. Seyedin, A.L. Stoltzfus, A.S. Levitt, M. Alhabeb, M. Anayee, C. J. Strobel, J.M. Raza, G. Dion, Y. Gogotsi, Knittable and washable multifunctional MXene-coated cellulose yarns, *Adv. Funct. Mater.* 29 (45) (2019), 1905015.
- [218] Y. Yu, G. Zheng, K. Dai, W. Zhai, K. Zhou, Y. Jia, G. Zheng, Z. Zhang, C. Liu, C. Shen, Hollow-porous fibers for intrinsically thermally insulating textiles and wearable electronics with ultrahigh working sensitivity, *Mater. Horiz.* 8 (3) (2021) 1037–1046.
- [219] T. Yamada, Y. Hayamizu, Y. Yamamoto, Y. Yomogida, A. Izadi-Najafabadi, D. N. Futaba, K. Hata, A stretchable carbon nanotube strain sensor for human-motion detection, *Nat. Nanotechnol.* 6 (5) (2011) 296–301.
- [220] J. Eom, R. Jaisutti, H. Lee, W. Lee, J.-S. Heo, J.-Y. Lee, S.K. Park, Y.-H. Kim, Highly sensitive textile strain sensors and wireless user-interface devices using all-polymeric conducting fibers, *ACS Appl. Mater. Interfaces* 9 (11) (2017) 10190–10197.

- [221] J. Lee, S. Shin, S. Lee, J. Song, S. Kang, H. Han, S. Kim, S. Kim, J. Seo, D. Kim, T. Lee, Highly sensitive multifilament fiber strain sensors with ultrabroad sensing range for textile electronics, *ACS Nano* 12 (5) (2018) 4259–4268.
- [222] Z. Wang, Y. Huang, J. Sun, Y. Huang, H. Hu, R. Jiang, W. Gai, G. Li, C. Zhi, Polyurethane/cotton/carbon nanotubes core-spun yarn as high reliability stretchable strain sensor for human motion detection, *ACS Appl. Mater. Interfaces* 8 (37) (2016) 24837–24843.
- [223] C.B. Cooper, K. Arutselvan, Y. Liu, D. Armstrong, Y. Lin, M.R. Khan, J. Genzer, M. D. Dickey, Stretchable capacitive sensors of torsion, strain, and touch using double helix liquid metal fibers, *Adv. Funct. Mater.* 27 (20) (2017), 1605630.
- [224] M. Amjadi, K.-U. Kyung, I. Park, M. Sitti, Stretchable, skin-mountable, and wearable strain sensors and their potential applications: a review, *Adv. Funct. Mater.* 26 (11) (2016) 1678–1698.
- [225] Z. Wu, L. Wei, S. Tang, Y. Xiong, X. Qin, J. Luo, J. Fang, X. Wang, Recent progress in Ti3C2Tx MXene-based flexible pressure sensors, *ACS Nano* 15 (12) (2021) 18880–18894.
- [226] Y. Niu, H. Liu, R. He, Z. Li, H. Ren, B. Gao, H. Guo, G.M. Genin, F. Xu, The new generation of soft and wearable electronics for health monitoring in varying environment: from normal to extreme conditions, *Mater. Today* 41 (2020) 219–242.